Semialgebraic Convex Bodies

Von der Fakultät für Mathematik und Informatik
der Universität Leipzig
angenommene

D I S S E R T A T I O N

zur Erlangung des akademischen Grades

DOCTOR RERUM NATURALIUM
(Dr.rer.nat.)

im Fachgebiet

Mathematik

vorgelegt

von M.Sc. Chiara Meroni
geboren am 22.01.1996 in Gorizia (Italien)

Contents

Chapter 1

Introduction

Convex Geometry has been classically studied from an analytical point of view. To convex sets, one can associate appropriate functions and measures, study regularity and inequalities, in the interplay between functional analysis, harmonic analysis and probability. On the other hand, polyhedra are also naturally connected to combinatorics, linear algebra and linear programming. This has been the starting point for the development of the field of Convex Algebraic Geometry, which focuses mainly on semidefinite optimization, dealing for instance with spectrahedra and sums of squares.

This work aims to taking a further step toward the connection between the two communities of convex and algebraic geometry. The underlying theme is indeed to approach the study of convex bodies using tools from real and complex algebraic geometry. For this to be meaningful, one should dive into the realm of semialgebraic convex bodies, which are convex compact subsets of a Euclidean space defined by a Boolean combination of polynomial inequalities. One of the main characters that will guide us throughout the text is the algebraic boundary. It is defined to be the smallest complex algebraic variety that contains the topological boundary of a convex body. This procedure allows us to associate a variety to a convex body, and thereby to get information about the latter via algebraic geometry.

[Describe here the structure of the thesis]

Chapter 2

Background

In this chapter we will start by introducing basic notions in convex geometry, that will be useful in later chapters. For extended discussions and proofs we refer to Schneider's book [Sch13] and Barvinok's book [Bar02]. The second section is devoted to review relevant definitions and results regarding semialgebraic convex bodies, based mainly on [Sin15]. We will also recall some machineries from (real) algebraic geometry.

2.1. Basics of Convex Geometry

[Improve and add precise citations]

To start talking about convex geometry, we shall introduce the notion of convex set. Throughout the thesis we will always work in a Euclidean space, therefore we give all the definitions in this setting, even though some make sense more in general. A set $A \subset \mathbb{R}^d$ is said to be *convex* if for every pair of points $x, y \in A$ the whole segment between them is contained in A. More precisely, given two points $x, y \in \mathbb{R}^d$ the segment between them is the set of all their convex combinations, namely

$$[x, y] = \{\alpha x + (1 - \alpha)y \,|\, \alpha \in [0, 1]\}.$$

The *dimension* of a convex set A is meant to be its dimension as topological space. Equivalently, it is the (vector space) dimension of the linear span of A. We will focus here on a specific class of convex sets.

Definition 2.1.1. A set $K \subset \mathbb{R}^d$ is called a *convex body* if it is a convex compact non-empty set. We denote the family of convex bodies of $\mathbb{R}^d$ by $\mathcal{K}(\mathbb{R}^d)$.

The intersection of convex sets is convex; the intersection of convex bodies is a convex body. Convexity is a very geometric, visual, intuitive condition and it is indeed easy to construct examples or counterexamples of convex sets and convex bodies. A ball is a convex body, a circle is not convex, a halfspace is convex but not a convex body; in $\mathbb{R}$ a set is convex if and only if it is a line segment. Since not every set is convex, we need an operation to "convexify": this is the *convex hull*. The convex hull of $A \subset \mathbb{R}^d$ is the smallest convex set containing A, or alternatively it is the set of all convex combinations of points of A; in formula

$$\operatorname{conv} A = \left\{\alpha_1 x_1 + \ldots + \alpha_n x_n \,|\, x_1, \ldots, x_n \in A, \alpha_1, \ldots \alpha_n \in [0, 1], \sum_{i=1}^{n} \alpha_i = 1\right\}.$$

In particular, if $A \subset \mathbb{R}^d$ is compact, then $\mathrm{conv}\, A$ is a convex body. An important family of convex bodies can be defined using the notion of convex hull.

Definition 2.1.2. A *polytope* is the convex hull of finitely many points.

Polytopes appear in an extraordinary number of mathematical areas and have applications that go in many directions, from optimization, to life sciences, to physics (we will have a glimpse of this in Chapter 6). This should suggest that the literature on polytopes is huge and here we will just introduce few basic concepts that are relevant for later chapters. For a more deep and accurate introduction on this subject, proofs and exercises, we refer to Ziegler's book [Zie12]. Another object, intimately related to polytopes is the following.

Definition 2.1.3. Let $a_1, \ldots, a_n \in \mathbb{R}^d$ and $b_1, \ldots, b_n \in \mathbb{R}$. The set

$$\left\{ x \in \mathbb{R}^d \,|\, \langle a_i, x \rangle \geq b_i \text{ for all } i = 1, \ldots, n \right\}$$

is a *polyhedron*.

Polyhedra are intersections of halfspaces, hence they are convex. The following is know as Weyl-Minkowski's Theorem, also called the "Main theorem for polytopes" by Ziegler.

Theorem 2.1.4. A subset $P \subset \mathbb{R}^d$ is a polytope if and only if it is a bounded polyhedron.

This result provides two equivalent, dual (in a sense that will be made precise later) characterizations of a polytope. Definition 2.1.2 is called the *v*-representation of a polytope (the name will be clear later), whereas its description as a bounded polyhedron is the *h*-representation, since we are intersecting halfspaces defined by the hyperplanes. It is very useful to work with both definitions for proving statements. There are also other equivalent characterizations of a polytope, see cite precise theorem Ziegler. The family of polytopes is closed with respect to many operations: the intersection of two polytopes is a polytope, the projection of a polytope is a polytope, the convex hull of polytopes is a polytope.

There are other important operations allowed on $\mathcal{K}(\mathbb{R}^d)$:

- dilation: $\lambda K = \{\lambda x \,|\, x \in K\}$, for $\lambda \geq 0$, $K \in \mathcal{K}(\mathbb{R}^d)$,

- Minkowski sum: $K_1 + K_2 = \{x_1 + x_2 \,|\, x_i \in K_i \text{ for } i = 1, 2\}$, for $K_1, K_2 \in \mathcal{K}(\mathbb{R}^d)$.

The family of polytopes is closed with respect to these operations too. Combining them, we can turn the set of convex bodies into a metric space. One possible way is to use the *Hausdorff metric*. Given two convex bodies $K_1, K_2 \in \mathcal{K}(\mathbb{R}^d)$ define their Hausdorff distance to be

$$\mathrm{dist}_H(K_1, K_2) = \min\{\lambda \,|\, K_1 \subset K_2 + \lambda B^d \text{ and } K_2 \subset K_1 + \lambda B^d\}$$

where B^d is the unit d-dimensional ball. This is in fact a metric and $(\mathcal{K}(\mathbb{R}^d), \mathrm{dist}_H)$ is a complete metric space. We are now allowed to talk about density and limits, and whenever we will talk about a metric property of a convex body, even if not specified, we will always refer to the Hausdorff metric. A first remark is that polytopes are dense in $\mathcal{K}(\mathbb{R}^d)$. Therefore, given any convex body $K \subset \mathbb{R}^d$ and given $\varepsilon > 0$ there exists a polytope $P \subset \mathbb{R}^d$ such that $\mathrm{dist}_H(K, P) \leq \varepsilon$.

2.1.1. Face structure

What do people study about convex bodies? One of the (many!) possible answers is: the boundary. It is also one of the main focus of this thesis. If $A \subset \mathbb{R}^d$, we denote its

topological boundary by ∂A. We want to establish a systematic way to describe and talk about the boundary of a convex body. This can be done via the notion of faces.

Definition 2.1.5. A convex subset $F \subset K$ of a convex body is a *face* if $x, y \in K$ and $\frac{x+y}{2} \in F$ implies $x, y \in F$. If a point $\{x\}$ is a face of K, it is called *extreme point*. If K has dimension d and $\dim F = d - 1$, then F is called *facet*.

In particular, a point $x \in K$ is extreme if for every convex combination $x = \alpha y + (1-\alpha)z$ with $y, z \in K$, then $y = z = x$. The union of all the faces of a convex body is its topological boundary. If all the boundary points are extreme points, then we say that K is *strictly convex*. In this case the are no segments contained in ∂K, or equivalently it is a manifold with strictly positive curvature at all points. We can refine the notion of face as follows. Let $\langle \cdot, \cdot \rangle$ be the standard scalar product of $\mathbb{R}^d$; we use it throughout the whole thesis to identify the Euclidean space and its dual. Nevertheless, we will try to be consistent with the notation, using $x, y, z, \ldots$ for the original space and $u, v, w, \ldots$ for the dual.

Definition 2.1.6. Let $K \in \mathcal{K}(\mathbb{R}^d)$ and let $u \in \mathbb{R}^d$. The *face of K exposed by u* is the convex set

$$K^u = \{x \in K \mid \langle u, x \rangle \geq \langle u, y \rangle \text{ for all } y \in K\}.$$

We will also say that K^u is the face of K exposed by u. If a point $\{x\}$ is an exposed face of K, it is called *exposed point*.

Such a vector $u \in \mathbb{R}^d$ corresponds, via the scalar product, to a linear functional $u \in (\mathbb{R}^d)^*$, that with abuse of notation we denote again by u. In this language, K^u is the set of points of K where the linear functional u attains its maximum over K. Geometrically, an exposed face arises as the intersection of K with a so called *separating hyperplane*: it is a hyperplane H such that K is contained in one of the two (closed) halfspaces identified by H, with $H \cap K \neq \emptyset$. Such a hyperplane is parallel to $u^\perp$, the orthogonal complement of u. Notice that an exposed face is a face, but a face need not to be exposed. In particular, we will denote the set of extreme points of K by $\partial_e(K)$ and the set of its exposed points by $\mathrm{Exp}(K)$. The set of extreme points contains the set of exposed points, but it is not much bigger: every extreme point is a limit (in the Euclidean topology) of exposed points.

Example 2.1.7. Consider the convex body in Figure 2.1, namely

$$K = \mathrm{conv}\left\{ \{(x \pm 1)^2 + (y - 1)^2 = 1\} \cup \{(0, -1 - \frac{1}{\sqrt{2}})\} \right\}.$$

The four points $(\pm 1, 2), \left(\pm (1 + \frac{1}{\sqrt{2}}), 1 - \frac{1}{\sqrt{2}} \right)$ are extreme but not exposed. They belong to one of the facets exposed by the vectors $(0, 1), (\pm 1, -1)$. The set of exposed points is the union of two (open) arcs and a point, whereas the extreme points are

$$\partial_e(K) = \mathrm{Exp}(K) \cup \left\{ (\pm 1, 2), \left(\pm (1 + \frac{1}{\sqrt{2}}), 1 - \frac{1}{\sqrt{2}} \right) \right\}.$$

K is not strictly convex since there are three segments contained in the boundary: they are the facets of K. ◆

In a way, the extreme points contain all the information regarding a convex body. This is made precise by a result obtained by Krein and Milman, proved in more generality in [KM40], which is also known as Minkowski's Theorem.

Theorem 2.1.8. Let $K \in \mathcal{K}(\mathbb{R}^d)$. Then K is the convex hull of the set of its extreme points. In formula, $K = \mathrm{conv}(\partial_e(K))$.

Remark that taking the convex hull of the extreme points is the best we can do: for every subset $A \subsetneq \partial_e(K)$ we have that $\mathrm{conv}(A) \subsetneq K$. In the case of polytopes things
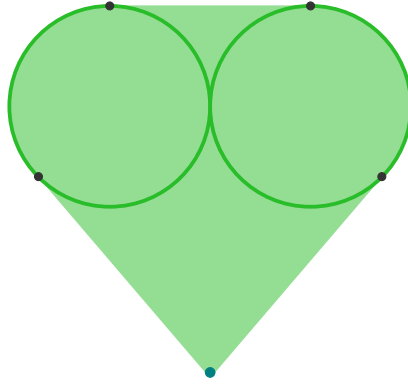
Figure 2.1: The convex hull of two circles and a point. The four black dots are extreme, non-exposed points.

simplifies a bit: all faces are exposed and every face is the convex hull of finitely many points, hence a polytope again. The fallout is that polytopes have finitely many faces, that we can store in the *f-vector* $(f_0, \ldots, f_{d-1})$. The $f_i(P)$ is the number of i-th dimensional faces of P.

The counterparts of the faces of a convex body are the normal cones. A convex cone is a set $C \subset \mathbb{R}^d$ such that if $x \in C$ then $\lambda x \in C$ for all $\lambda \geq 0$. In particular, a cone is unbounded, hence it is not a convex body. Also in this case, we can turn any set A into a cone by considering its *conic hull* co$A$, which is defined to be the smallest convex cone containing A.

Given a point $x \in K$, the *normal cone* to $x \in K$ is the convex cone

$$\mathsf{N}_K(x) = \left\{ u \in \mathbb{R}^d \,|\, \langle u, x \rangle \geq \langle u, y \rangle \text{ for all } y \in K \right\}.$$

This is the set of all vectors that expose a face of K containing x, so it also makes sense to talk about the normal cone $\mathsf{N}_K(F)$ *to a face F* of K. The correspondence $F \mapsto \mathsf{N}_K(F)$ is an inclusion-reversing operation. By the linearity of the scalar product, normal cones are convex cones, but their dimension can vary.

Definition 2.1.9. Let $K \in \mathcal{K}(\mathbb{R}^d)$ be a full dimensional convex body. An extreme point $x \in \partial K$ is a *vertex* if $\dim \mathsf{N}_K(x) > 1$.

If the convex body is a polytope $P \subset \mathbb{R}^d$, the normal cone to a face F has dimension $d - \dim F$, so all the extreme points are vertices. This justifies the letter "v" in the v-representation of Definition 2.1.2. In this case, the union of all normal cones is a complete fan [Zie12, Definition 7.1], called the *normal fan* of P.

In Example 2.1.7 the normal cone at $x = \left(0, -1 - \frac{1}{\sqrt{2}}\right)$ is the two-dimensional set

$$\mathsf{N}_K(x) = \text{co} \left\{ (\pm 1, -1) \right\},$$

hence x is a vertex of K. At all the other points of ∂K the normal cone is a ray. Notice that the two vectors $(\pm 1, -1)$ already appeared in our example, and it is not a coincidence. In order to exploit such structure we should define an object that encodes information about K, its normal cones and its exposed faces.
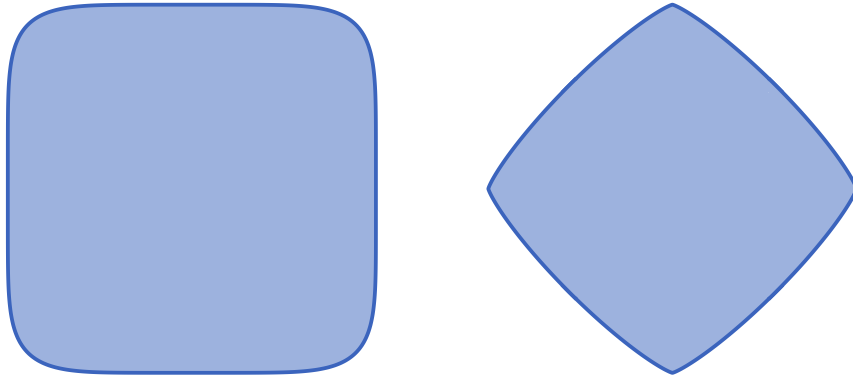
Figure 2.2: Left: the L_6 unit ball. Right: the $L_{\frac{6}{5}}$ unit ball.

2.1.2. Duality in convex geometry

In this section we introduce the first constructions with convex bodies, a theme that will come back in Section 4. The general philosophy consists in manipulating a convex body K in order to create a new object (another convex body for instance) and study the relations among the former and the latter.

Definition 2.1.10. Let $K \in \mathcal{K}(\mathbb{R}^d)$. The *dual* (or polar) convex body of K is

$$K^\circ = \left\{ u \in \mathbb{R}^d \,|\, \langle u, x \rangle \leq 1 \text{ for all } x \in K \right\}.$$

Formally, the dual body would live in the dual space $(\mathbb{R}^d)^*$ that we are identifying with $\mathbb{R}^d$. Note that in the literature there are different definitions of the dual body: here we are using the convention with *outer* normal vectors. Directly from the definition, one can prove that this duality is an inclusion-reversing operation on convex bodies and that it almost commutes with linear transformations: given $g \in GL_d(\mathbb{R})$ we have that $(g \cdot K)^\circ = g^{-T} \cdot K^\circ$. Another immediate observation is that K° is always a convex body that contains the origin. This leads to the Bidual (or Bipolar) Theorem.

Theorem 2.1.11. Let $K \in \mathcal{K}(\mathbb{R}^d)$ such that $0 \in K$. Then $K^{\circ\circ} = K$.

More in general $K^{\circ\circ} = \mathrm{conv}\{K \cup 0\}$. We will usually use the expression "dual body" instead of "polar" in order to emphasize that this is a duality operation. Moreover, it is linked to other notions of duality, as we will discuss in the following example and also in Section 2.2.

Example 2.1.12. Let $K \subset \mathbb{R}^d$ be the L_p unit ball of $\mathbb{R}^d$. It is a convex body. Using Hölder's inequality one can prove that its dual body is the L_q unit ball, where $\frac{1}{p} + \frac{1}{q} = 1$. Figure 2.2 shows the case $d = 2$, $p = 6$, $q = \frac{6}{5}$. ⧫

The polytopal case is again special: the dual body of a polytope is a polytope itself. In particular, the v-representation of P becomes the h-representation of P°, and conversely. We highlight this with an example.

Example 2.1.13. Let $P = [-1, 1]^4$ be the four-dimensional cube centred at the origin. Its dual polytope is

$$P^\circ = \left\{ u \in \mathbb{R}^d \,|\, \langle u, v_i \rangle \leq 1 \right\}.$$

The vertices of P° are the eight points $(\pm 1, 0, 0, 0), (0, \pm 1, 0, 0), (0, 0, \pm 1, 0), (0, 0, 0, \pm 1),$

which are exactly the vectors that give the linear inequalities in the definition of P (i.e., they are the a_i's of Definition 2.1.3). ◆

The construction of the dual convex body induces an analogous notion on faces. Let F be a face of K, and define its *dual face* F° to be the set of linear functionals that attain their maximum over K at F. In the nice case in which the origin lies in the interior of K, one has

$$F^\circ = \left\{ u \in \mathbb{R}^d \,|\, \langle u, x \rangle = 1 \text{ for all } x \in F \right\}.$$

The dual face is always an exposed face by definition, and we can also recover all the exposed faces in this way. This is made precise by the following statement, a version of biduality for faces.

Corollary 2.1.14. Let $K \in \mathcal{K}(\mathbb{R}^d)$ such that $0 \in K$. Let F be an exposed face of K. Then $F^{\circ\circ} = F$.

When the convex body is a polytope P, all faces are exposed and the dual face to F is just the intersection of $\mathsf{N}_P(F)$ with the hyperplane $\langle u, x \rangle = 1$. Hence, we always have that

$$\dim F + \dim F^\circ = d - 1. \tag{2.1.1}$$

In particular, vertices of P correspond to facets of P°, edges of P correspond to faces of P° of dimension $d - 2$, and so on. We can translate this observation in terms of the f-vector: $f_i(P) = f_{d-1-i}(P)$ for a full dimensional polytope $P \subset \mathbb{R}^d$. Equation (2.1.1) does not hold for more general convexbodies. For instance, consider the L_6 unit ball displayed in Figure 2.2, left. Since it is strictly convex, all the points in its boundary are faces. In this case, all faces are actually exposed and they are always exposed by a unique vector. So we have that $\dim F + \dim F^\circ = 0 < 1$ for every face.

The normal cycle. The definition of the polar suggests to look at the *incidence relation* between points $x \in K$ and $u \in K^\circ$ for which the inequality $\langle u, x \rangle \leq 1$ is tight. The resulting set is called the normal cycle.

Definition 2.1.15. Let $K \in \mathcal{K}(\mathbb{R}^d)$ with the origin in its interior. The *normal cycle* of K is defined as

$$\mathbf{N}(K) = \left\{ (x, u) \in \partial K \times \partial K^\circ \,|\, \langle x, u \rangle = 1 \right\}.$$

This integrates K and K° into a single structure, but it is useful far beyond this role. Fixing x to range over a face $F \subset \partial K$ leaves u to range over the exposed face F° of K°.

Let us look at the two extreme cases of convex sets: first, we have strictly convex sets with smooth boundary, whose only faces are exposed points. Here, $\mathbf{N}(K)$ is the graph of a homeomorphic identification of ∂K with ∂K°. If on the other hand K is a polytope, although the normal cycle is far from being a convex set, for every k-dimensional face F, the set $F \times F^\circ \subset \mathbf{N}(K)$ is a polytope of dimension $k + (d - k - 1) = d - 1$.

Example 2.1.16. Consider the four-dimensional cube $P = [-1, 1]^4$ from Example 2.1.3 and its dual polytope P°. Their f-vectors are $(16, 32, 24, 8)$ and $(8, 24, 32, 16)$ respectively. The common (up to relabelling the coordinates) normal cycle $\mathbf{N}(P) = \mathbf{N}(P^\circ)$ consists of 80 strata (this word will make precise later, for now just think of them as pieces, building blocks), one for each of the $16 + 32 + 24 + 8$ pairs (F, F°), where $F \subset \partial P$ and $F^\circ \subset \partial P^\circ$ are faces of complement dimension. For instance, if $\dim(F) = 1$ then F° is a triangle and $F \times F^\circ$ is a triangular prism. ◆

The power of the normal cycle lies in the uniform treatment covering the whole range of convex bodies from polytopes to smooth. Indeed, for any compact convex d-dimensional

set K containing the origin in its interior, $\mathbf{N}(K)$ is always a $(d-1)$-dimensional (Lipschitz Legendrian) submanifold of $\mathbb{R}^{2d}$ [Fu14]. Moreover, the map $K \mapsto \mathbf{N}(K)$ is continuous in the Hausdorff metric for sets. This makes the normal cycle a remarkably stable structure under approximations either by smooth manifolds or by polytopes.

The normal cycle plays the role of the normal bundle for more general geometric objects. It was defined by Federer [Fed59] for sets of positive reach. These include convex bodies but also much crazier sets. It is an important tool from geometric measure theory, used for defining curvature measures [Win82, Zäh86]. This is related to the classic result of Steiner, who noted that the volume of the smooth approximation to a body, which one gets as the union of all balls of small radius r centered on the body, is a polynomial in r, whose coefficients relate to curvature of different dimensionality. On the other hand, stable polyhedral approximations are needed in visualization, computer graphics and computational anatomy (see [CSM03, RG17, SLC$^+$19]). Recently, the normal cycle has also emerged as a key player in convex algebraic geometry [CKLS19, PSW21] as we will see in Section 2.2.

2.1.3. Functions and convex bodies

One of the reasons why polytopes are popular is that they have finite descriptions, as we highlighted for instance with the v and the h-representations. As soon as one moves away from polytopes, these finiteness properties are not true any more. Therefore one needs to find another efficient way to describe a convex body. This can be done using several functions (for details see [Sch13, Section 1.7]).

Definition 2.1.17. The *support function* of a convex body K is $h_K : \mathbb{R}^d \to \mathbb{R}$ such that

$$h_K(u) = \max \left\{ \langle u, x \rangle \mid x \in K \right\}. \tag{2.1.2}$$

As the name suggests, it is related to the separating hyperplanes of K. In particular, the value of $h_K(u)$ is the (signed) distance to the origin of the supporting hyperplane with outer normal vector u. This implies that $\langle u, x \rangle \leq h_K(u)$ for every $x \in K$. We also get an alternative description of the exposed faces of K:

$$K^u = \left\{ x \in K \mid \langle u, x \rangle = h_K(u) \right\}.$$

Playing with the definition, one can discover that the support function is sublinear, i.e., $h_K(\lambda u) = \lambda h_K(u)$ for all $\lambda \geq 0$, and $h_K(u+v) \leq h_K(u) + h_k(v)$. In fact, all sublinear functions are support functions.

Theorem 2.1.18. Let $h : \mathbb{R}^d \to \mathbb{R}$ be a sublinear function. Then there exists a unique convex body $K \in \mathcal{K}(\mathbb{R}^d)$ such that $h_k = h$.

Therefore a convex body is uniquely identified by its support function. Endowing the space of convex bodies with the Hausdorff metric, we can think of the support function as $h : \mathcal{K}(\mathbb{R}^d) \times \mathbb{R}^d \to \mathbb{R}$ and it is a continuous function in both arguments. Also, we can use it to express the Hausdorff distance between two convex bodies:

$$\text{dist}_H(K_1, K_2) = \sup_{u \in S^{d-1}} |h_{K_1}(u) - h_{K_2}(u)|.$$

We summarize further properties of the support function in the following proposition.

Proposition 2.1.19. Let $K_1, K_2 \in \mathcal{K}(\mathbb{R}^d)$ with their respective support functions h_{K_1}, h_{K_2}. Then

(i) $h_{\lambda K_1} = \lambda h_{K_1}$;

(ii) $h_{K_1+K_2} = h_{K_1} + h_{K_2}$;

(iii) If $T : \mathbb{R}^d \to \mathbb{R}^k$ is a linear map then $h_{TK} = h_K \circ T^t$;

(iv) h_K is differentiable at $u \in \mathbb{R}^d$ if and only if the point x realizing the maximum in (2.1.2) is unique. In that case $x = K^u = \nabla h_K(u)$, where ∇h_K denotes the gradient of h_K.

Recognizing a convex body from its support function is not always easy, but there are some cases in which it is possible. The convex body is a polytope if and only if h_K is piecewise linear; in particular $h_K(\cdot) = \langle \cdot, x \rangle$ if and only if $K = \{x\}$. The support function of the ball of radius r centred at the origin looks like $h_{rB^d}(u) = r\|u\|$.

Another function that will be useful later in Section 4.2 is the radial function.

Definition 2.1.20. Let $K \in \mathcal{K}(\mathbb{R}^d)$ containing the origin. Its *radial function* is $\rho_K : \mathbb{R}^d \to \mathbb{R}$ such that
$$\rho_K(x) = \max\{\lambda \geq 0 \mid \lambda x \in K\}. \tag{2.1.3}$$

Radial functions are actually meaningful for a larger class of sets: the starshaped sets. A set $A \subset \mathbb{R}^d$ is *starshaped* if there exists $x_0 \in A$ such that for all $x \in K$ we have $[x_0, x] \subset A$. Convex sets are starshaped with respect to any of their points. We assume from now when talking about starshaped set that they are starshaped with respect to the origin, i.e., $x_0 = 0$. Then, compact starshaped sets have an associated radial function as defined in (2.1.3). This function satisfies $\rho_K(\lambda x) = \frac{1}{\lambda}\rho_K(x)$ for all $\lambda > 0$, hence it is enough to define it on the unit sphere. Given the radial function ρ, we can recover the associated starshaped set and its topological boundary (when that the origin lies in the interior of A):

$$A = \left\{ x \in \mathbb{R}^d \mid \rho(x) \geq 1 \right\}, \quad \partial A = \left\{ x \in \mathbb{R}^d \mid \rho(x) = 1 \right\}.$$

Let K be a convex body with the origin in its interior. Its support and radial functions are related to each other via duality, namely

$$h_K(u) = \frac{1}{\rho_{K^\circ}(u)}, \quad \rho_K(u) = \frac{1}{h_{K^\circ}(u)}.$$

As a consequence, we can describe the boundary of the dual body K° as the set of points $x \in \mathbb{R}^d$ such that $h_K(u) = 1$.

2.2. Varieties and Convex Bodies

Chapter 3

Zonoids

3.1. Zonoids and their problems

3.2. Discotopes

Chapter 4

Constructions with Convex Bodies

Many areas of convex geometry investigate objects that are defined starting from a convex body. We considered here two particular constructions: fiber convex bodies and intersection bodies.

If K is a convex body in $\mathbb{R}^{n+m}$ and $\pi : \mathbb{R}^{n+m} \to V$ is the orthogonal projection onto a subspace $V \subset \mathbb{R}^{n+m}$ of dimension n, the fiber body of K with respect to π is the *average* of the fibers of K under this projection:

$$\Sigma_\pi K = \int_{\pi(K)} \left(K \cap \pi^{-1}(x) \right) \mathrm{d}x. \qquad (4.0.1)$$

This expression will be made rigorous in Proposition 4.1.6.

Such notion was introduced for polytopes by Billera and Sturmfels in [BS92]. It has been investigated in many different contexts, from combinatorics such as in [ADRS00] to algebraic geometry and even tropical geometry in the context of polynomial systems [EK08, Est08, SY08]. Notably, recent studies concern the particular case of monotone path polytopes [BL21].

We focus here on the study of the fiber body of convex bodies that are not polytopes. We introduce and study the general properties of these objects. Then, we devote three subsections to the analysis of the fiber body of three particular classes of convex bodies.

Subsection 4.1.1 concerns the *puffed polytopes*. They are convex bodies that are obtained from polytopes by taking the "derivative" of their algebraic boundary (see Definition 4.1.14). Propositions 4.1.19, 4.1.20 and 4.1.21 describe the strict convexity of the fiber body of a puffed polytope. As a concrete example we study the case of the elliptope and a particular projection.

In Subsection 4.1.2 we investigate the class of curved convex bodies. Namely, we consider convex bodies whose boundary is a C^2 hypersurface with a strictly positive curvature. In that case Theorem 4.1.26 gives an explicit formula for the support function of $\Sigma_\pi K$, directly in terms of the support function of K. This is an improvement of equation (4.1.2) which involves the support function of the fibers. We give an example in which the support function of the fiber body is easily computed using Theorem 4.1.26.

The last subsection of Section 4.1 is dedicated to the case of zonoids. We prove that the fiber body of a zonoid is a zonoid, and give an explicit formula to compute it in Theorem 4.1.37. We then exhibit an example of a semialgebraic convex body, the Dice, that has a fiber body which is not semialgebraic. Hence, semialgebraicity is not preserved by the operation of computing the fiber body.

Section 4.2 focuses on intersection bodies of polytopes, from the perspective of real algebraic geometry. Originally, intersection bodies were defined by Lutwak [Lut88] in the context of convex geometry. In view of the notion of $(d-1)$-dimensional cross-section measures and the related concepts of associated bodies (such as intersection bodies, cross-section bodies, and projection bodies), intersection bodies play an essential role in geometric tomography (see [Gar06, Chapter 8] and [Mar94, Section 2.3]). In particular, we mention here the Busemann-Petty problem which asks if one can compare the volumes of two convex bodies by comparing the volumes of their sections [Gar94a, Gar94b, GKS99, Kol98, Zha99b]. Moreover, Ludwig showed that the unique non-trivial $GL(d)$-covariant star-body-valued valuation on convex polytopes corresponds to taking the intersection body of the dual polytope [Lud06]. Due to such results, the knowledge on properties of intersection bodies interestingly contributes also to the (still not systematized) theory of starshaped sets, see Section 17 of the exposition [HHMM20].

We study here intersection bodies of polytopes from a geometric and algebraic perspective. It is known that in $\mathbb{R}^2$, the intersection body of a centrally symmetric polytope centered at the origin is the same polytope rotated by $\pi/2$ and dilated by a factor of 2 (see e.g. [Gar06, Theorem 8.1.4]). Moreover, if K is a full-dimensional convex body in $\mathbb{R}^d$ centered at the origin, then so is its intersection body [Gar06, Chapter 8.1]. But what do these objects look like in general? In $\mathbb{R}^d$, with $d \geq 3$, they cannot be polytopes [Cam99, Zha99a] and they may not even be convex. In fact, for every convex body K, there exists a translate of K such that its intersection body is not convex. This happens because of the important role played by the origin in this construction.

Our main contribution is Theorem 4.2.10, which states that the intersection body of a polytope is a semialgebraic set. The proof relies on two key facts. First, the volume of a polytope can be computed using determinants. Second, the combinatorial type of the intersection of a polytope with a hyperplane is fixed for each region of a certain central hyperplane arrangement. We first prove the semialgebraicity of the intersection body of polytopes containing the origin, and we generalize the result to arbitrary polytopes in 4.2.1. In 4.2.2, we present an algorithm to compute the radial function of the intersection body of a polytope. An implementation is available at [Mat21]. In 4.2.3, we describe the algebraic boundary of the intersection body, which is a hypersurface consisting of several irreducible components, each corresponding to a region of the aforementioned hyperplane arrangement. 4.2.16 gives a bound on the degree of the irreducible components. 4.2.4 focuses on the intersection body of the d-cube centered at the origin (4.9a).

4.1. Fiber Convex Bodies

Consider the Euclidean vector space $\mathbb{R}^{n+m}$ endowed with the standard Euclidean structure and let $V \subset \mathbb{R}^{n+m}$ be a subspace of dimensions n. Denote by W its orthogonal complement, such that $\mathbb{R}^{n+m} = V \oplus W$. Let $\pi : \mathbb{R}^{n+m} \to V$ be the orthogonal projection onto V. Throughout this section we will canonically identify the Euclidean space with its dual. However the notation is meant to be consistent: x, y, z will denote vectors, whereas we will use u, v, w for dual vectors.

If $K \in \mathcal{K}(\mathbb{R}^{n+m})$ we write K_x for the orthogonal projection onto W of the fiber of $\pi|_K$ over x, namely

$$K_x := \{y \in W \mid (x, y) \in K\}.$$

Definition 4.1.1. Consider $\gamma : \pi(K) \to W$ such that for all $x \in \pi(K)$, $\gamma(x) \in K_x$. Such map is called a *section of π*, or just *section* when there is no ambiguity.

Using this notion we are able now to define our object of study. Notice that the word *measurable* is always intended with respect to the Borelians.

Definition 4.1.2. The *fiber body* of K with respect to the projection π is the convex body

$$\Sigma_\pi K := \left\{ \int_{\pi(K)} \gamma(x)\,\mathrm{d}x \mid \gamma : \pi(K) \to W \text{ measurable section} \right\} \in \mathcal{K}(W).$$

Here $\mathrm{d}x$ denotes the integration with respect to the n–dimensional Lebesgue measure on V. We say that a section γ *represents* $y \in \Sigma_\pi K$ if $y = \int_{\pi(K)} \gamma(x)\mathrm{d}x$.

Remark 4.1.3. Note that, with this setting, if $\pi(K)$ is of dimension $< n$, then its fiber body is $\Sigma_\pi K = \{0\}$.

This definition of fiber bodies, that can be found for example in [Est08] under the name *Minkowski integral*, extends the classic construction of fiber polytopes [BS92], up to a constant. Here, we choose to omit the normalization $\frac{1}{\mathrm{vol}(\pi(K))}$ in front of the integral used by Billera and Sturmfels in order to make apparent the *degree* of the map Σ_π seen in (4.1.1). This degree becomes clear with the notion of *mixed fiber body*, see [Est08, Theorem 1.2].

Proposition 4.1.4. For any $\lambda \in \mathbb{R}$ we have $\Sigma_\pi(\lambda K) = \lambda|\lambda|^n \Sigma_\pi K$. In particular if $\lambda \geq 0$

$$\Sigma_\pi(\lambda K) = \lambda^{n+1} \Sigma_\pi K. \tag{4.1.1}$$

Proof. If $\lambda = 0$ it is clear that the fiber body of $\{0\}$ is $\{0\}$. Suppose now that $\lambda \neq 0$ and let $\gamma : \pi(K) \to W$ be a section. We can define another section $\tilde\gamma : \pi(\lambda K) \to W$ by $\tilde\gamma(x) := \lambda\gamma\left(\frac{x}{\lambda}\right)$. Using the change of variables $y = x/\lambda$, we get that

$$\int_{\lambda\pi(K)} \tilde\gamma(x)\,\mathrm{d}x = \lambda|\lambda|^n \int_{\pi(K)} \gamma(y)\,\mathrm{d}y.$$

This proves that $\Sigma_\pi \lambda K \subseteq \lambda|\lambda|^n \Sigma_\pi K$. Repeating the same argument for λ^{-1} instead of λ, the other inclusion follows. $\square$

Corollary 4.1.5. If K is centrally symmetric then so is $\Sigma_\pi K$.

Proof. Apply the previous proposition with $\lambda = -1$ to get $\Sigma_\pi((-1)K) = (-1)\Sigma_\pi K$. If K is centrally symmetric with respect to the origin then $(-1)K = K$ and the result follows. The general case is obtained by a translation. $\square$

As a consequence of the definition, it is possible to deduce a formula for the support function of the fiber body. This is the rigorous version of equation (4.0.1).

Proposition 4.1.6. For any $u \in W$ we have

$$h_{\Sigma_\pi K}(u) = \int_{\pi(K)} h_{K_x}(u)\mathrm{d}x. \tag{4.1.2}$$

Proof. By definition

$$h_{\Sigma_\pi K}(u) = \sup\left\{ \int_{\pi(K)} \langle u, \gamma(x)\rangle\,\mathrm{d}x \mid \gamma \text{ measurable section} \right\} \leq \int_{\pi(K)} h_{K_x}(u)\mathrm{d}x.$$

To obtain the equality, it is enough to show that there exists a measurable section $\gamma_u : \pi(K) \to W$ with the following property: for all $x \in \pi(K)$ the point $\gamma_u(x)$ maximizes the linear form $\langle u, \cdot\rangle$ on K_x. In other words for all $x \in \pi(K)$, $\langle u, \gamma_u(x)\rangle = h_{K_x}(u)$. This is due to [Aum65, Proposition 2.1]. $\square$

A similar result can be shown for the faces of the fiber body.

Definition 4.1.7. Let $K \in \mathcal{K}(\mathbb{R}^{n+m})$ and let $u \in \mathbb{R}^{n+m}$. We denote by K^u the face of K in direction u, that is all the points of K that maximize the linear form $\langle u, \cdot \rangle$:

$$K^u := \{y \in K \mid \langle u, y \rangle = h_K(u)\}.$$

Moreover, if $\mathcal{U} = \{u_1, \ldots, u_k\}$ is an ordered family of vectors of $\mathbb{R}^{n+m}$, we write

$$K^{\mathcal{U}} := (\cdots (K^{u_1})^{u_2} \cdots)^{u_k}.$$

We show that the face of the fiber body is, in some sense, the fiber body of the faces.

Lemma 4.1.8. Let $\mathcal{U} = \{u_1, \ldots, u_k\}$ be a an ordered family of linearly independent vectors of W, take $y \in \Sigma_\pi K$ and let $\gamma : \pi(K) \to W$ be a section that represents y. Then $y \in (\Sigma_\pi K)^{\mathcal{U}}$ if and only if $\gamma(x) \in (K_x)^{\mathcal{U}}$ for almost all $x \in \pi(K)$. In particular we have that

$$(\Sigma_\pi K)^{\mathcal{U}} = \left\{ \int_{\pi(K)} \gamma(x)\mathrm{d}x \mid \gamma \text{ section such that } \gamma(x) \in (K_x)^{\mathcal{U}} \text{ for all } x \right\}. \qquad (4.1.3)$$

Proof. Suppose first that $\mathcal{U} = \{u\}$. Assume that $\gamma(x)$ is not in $(K_x)^u$ for all x in a set of non–zero measure $\mathcal{O} \subset \pi(K)$. Then there exists a measurable function $\xi : \pi(K) \to W$ with $\langle u, \xi \rangle \geq 0$ and $\langle u, \xi(x) \rangle > 0$ for all $x \in \mathcal{O}$, such that $\tilde{\gamma} := \gamma + \xi$ is a section (for example you can take $\tilde{\gamma}(x)$ to be the nearest point on K_x of $\gamma(x) + u$). Let $\tilde{y} := \int_{\pi(K)} \tilde{\gamma}$. Then $\langle u, \tilde{y} \rangle = \langle u, y \rangle + \int_{\pi(K)} \langle u, \xi \rangle > \langle u, y \rangle$. Thus y does not belong to the face $(\Sigma_\pi K)^u$.

Suppose now that y is not in the face $(\Sigma_\pi K)^u$. Then there exists $\tilde{y} \in \Sigma_\pi K$ such that $\langle u, \tilde{y} \rangle > \langle u, y \rangle$. Let $\tilde{\gamma}$ be a section that represents $\tilde{y}$. It follows that $\int_{\pi(K)} \langle u, \tilde{\gamma} \rangle > \int_{\pi(K)} \langle u, \gamma \rangle$. This implies the existence of a set $\mathcal{O} \subset \pi(K)$ of non–zero measure where $\langle u, \tilde{\gamma}(x) \rangle > \langle u, \gamma(x) \rangle$ for all $x \in \mathcal{O}$. Thus for all $x \in \mathcal{O}$, $\gamma(x)$ does not belong to the face $(K_x)^u$.

In the case $\mathcal{U} = \{u_1, \ldots, u_{k+1}\}$ we can apply inductively the same argument. Replace $\Sigma_\pi K$ by $(\Sigma_\pi K)^{\{u_1, \ldots, u_k\}}$ and u by u_{k+1}, and use the representation of $(\Sigma_\pi K)^{\{u_1, \ldots, u_k\}}$ given by (4.1.3). $\qquad \square$

Using the same strategy in the proof of Proposition 4.1.6 we obtain the following formula.

Lemma 4.1.9. For every $u, v \in W$, $h_{(\Sigma_\pi K)^u}(v) = \int_{\pi(K)} h_{(K_x)^u}(v) \,\mathrm{d}x$.

The fiber body behaves well under the action of $\mathrm{GL}(V) \oplus \mathrm{GL}(W)$ as a subgroup of $\mathrm{GL}(\mathbb{R}^{n+m})$.

Proposition 4.1.10. Let $g_n \in \mathrm{GL}(V)$, $g_m \in \mathrm{GL}(W)$ and $K \in \mathcal{K}(\mathbb{R}^{n+m})$. Then

$$\Sigma_\pi\Big((g_n \oplus g_m)(K)\Big) = |\det(g_n)| \cdot g_m\Big(\Sigma_\pi K\Big).$$

Proof. This is a quite straightforward consequence of the definitions. After observing that

$$\Big((g_n \oplus g_m)(K)\Big)_x = g_m\Big(K_{g_n^{-1}(x)}\Big)$$

and $\pi((g_n \oplus g_m)(K)) = g_n\pi(K)$, use equation (4.1.2) with the change of variables $x \mapsto g_n^{-1}x$. By Proposition 2.1.19–(ii) we have $h_{g_m K_x}(u) = h_{K_x}(g_m^T u)$, so the thesis follows. $\qquad \square$
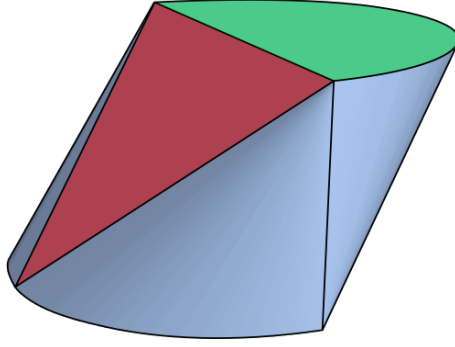
Figure 4.1: The convex body of Example 4.1.11. In its boundary there are 2 green half–discs, 2 red triangles and 4 blue cones.

Regularity of the sections. By definition, a point y of the fiber body $\Sigma_\pi K$ is the integral $y = \int_{\pi(K)} \gamma(x) \mathrm{d}x$ of a *measurable* section γ. Thus γ can be modified on a set of measure zero without changing the point y, i.e. y only depends on the L^1 class of γ. It is natural to ask what our favourite representative in this L^1 class will be and how regular can it be. In the case where K is a polytope, γ can always be chosen continuous. However if K is not a polytope and if y belongs to the boundary of $\Sigma_\pi K$, a continuous representative may not exists. This is due to the fact that in general the map $x \mapsto K_x$ is only upper semicontinuous, see [Kho12, Section 6].

Example 4.1.11. Consider the function $f : S^1 \to \mathbb{R}$ such that

$$f(x,y) = \begin{cases} 0 & x < 0 \\ 1 & x \geq 0 \end{cases}$$

and let $K := \mathrm{conv}(\mathrm{graph}(f)) \subset \mathbb{R}^3$ in Figure 4.1. This is a semialgebraic convex body, whose boundary may be subdivided in 8 distinct pieces: two half–discs lying on the planes $\{z = 0\}$ and $\{z = 1\}$, two triangles with vertices $(-1, 0, 0), (0, \pm 1, 1)$ and $(1, 0, 1), (0, \pm 1, 0)$ respectively, four cones with vertices $(0, \pm 1, 0), (0, \pm 1, 1)$. Let $\pi : \mathbb{R}^3 \to \mathbb{R}$ be the projection on the first coordinate $\pi(x, y, z) = x$. Then the point $p \in \Sigma_\pi K \subset \mathbb{R}^2$ maximizing the linear form associated to $(y, z) = (1, 0)$ must have only non–continuous sections. This can be proved using the representation of a face given by (4.1.3). ♦

We prove that most of the points of the fiber body have a continuous representative.

Proposition 4.1.12. Let $K \in \mathcal{K}(\mathbb{R}^{n+m})$ and let $\Sigma_\pi K$ be its fiber body. The set of its points that can be represented by a continuous section is convex and dense. In particular, all interior points of $\Sigma_\pi K$ can be represented by a continuous section.

Proof. Consider the set

$$C = \left\{ \int_{\pi(K)} \gamma(x) \mathrm{d}x \mid \gamma : \pi(K) \to K \text{ continuous section} \right\}$$

that is clearly contained in the fiber body $\Sigma_\pi K$. It is convex: take $a, b \in C$ represented by continuous sections $\alpha, \beta : \pi(K) \to K$ respectively. Then any convex combination can be written as $c = ta + (1-t)b = \int_{\pi(K)} \big(t\alpha(x) + (1-t)\beta(x) \big) dx$. Since $t\alpha + (1-t)\beta$ is a continuous section for any $t \in [0, 1]$, C is convex.

We now need to prove that the set C is also dense in $\Sigma_\pi K$. Let γ be a measurable section; by definition it is a measurable function $\gamma : \pi(K) \to W$, such that $\gamma(x) \in K_x$

for all $x \in \pi(K)$. For every $\epsilon > 0$ there exists a continuous function $g : \pi(K) \to W$ with $\|\gamma - g\|_{L^1} < \epsilon$, but this is not necessarily a section of K, since a priori $g(x)$ can be outside K_x. Hence define $\tilde{\gamma} : \pi(K) \to W$ such that

$$\tilde{\gamma}(x) = p\Big(K_x, g(x)\Big)$$

where $p(A, a)$ is the nearest point map at a with respect to the convex set A. By [Sch13, Lemma 1.8.11] $\tilde{\gamma}$ is continuous and by definition graph$(\tilde{\gamma}) \subset K$. Therefore $\int_{\pi(K)} \tilde{\gamma} \in C$. Moreover,

$$\|\gamma - \tilde{\gamma}\|_{L^1} \leq \|\gamma - g\|_{L^1} < \epsilon$$

hence the density is proved. As a consequence we get that $\mathrm{int}\Sigma_\pi K \subseteq C \subseteq \Sigma_\pi K$ so all the interior points of the fiber body have a continuous representative. $\square$

To our knowledge, the regularity of the sections needed to represent all points is not known.

Strict convexity.   In the case where K^u consists of only one point we say that K is *strictly convex in direction* u. Moreover, a convex body is said to be *strictly convex* if it is strictly convex in every direction. We now investigate this property for fiber bodies.

Proposition 4.1.13. Let $K \in \mathcal{K}(\mathbb{R}^{n+m})$ and let us fix a vector $u \in W$. The following are equivalent:

(i) $\Sigma_\pi K$ is strictly convex in direction u;

(ii) almost all the fibers K_x are strictly convex in direction u.

Proof. By Proposition 2.1.19–(iii), a convex body is strictly convex in direction u if and only if its support function is $\mathcal{C}^1$ at u. Therefore, if almost all the fibers K_x are strictly convex in u, then being the convex body compact, the support function $h_{\Sigma_\pi K}(u) = \int_{\pi(K)} h_{K_x}(u) \mathrm{d}x$ is $\mathcal{C}^1$ at u, i.e. the fiber body is strictly convex in that direction.

Now suppose that $\Sigma_\pi K$ is strictly convex in direction u, i.e. $(\Sigma_\pi K)^u$ consists of just one point y. This means that the support function of this face is linear and it is given by $\langle y, \cdot \rangle$. We now prove that the support function of K_x^u is linear for almost all x, and this will conclude the proof. Lemma 4.1.9 implies that

$$h_{(\Sigma_\pi K)^u} = \int_{\pi(K)} h_{K_x^u} \mathrm{d}x = \langle y, \cdot \rangle.$$

For any two vectors v_1, v_2, we have

$$\langle y, v_1 + v_2 \rangle = \int_{\pi(K)} h_{K_x^u}(v_1 + v_2) dx \leq \int_{\pi(K)} h_{K_x^u}(v_1) dx + \int_{\pi(K)} h_{K_x^u}(v_2) dx = \langle y, v_1 \rangle + \langle y, v_2 \rangle$$

thus the inequality in the middle must be an equality. But since $h_{K_x^u}(v_1 + v_2) \leq h_{K_x^u}(v_1) + h_{K_x^u}(v_2)$, we get that this is an equality for almost all x, i.e. the support function of K_x^u is linear for almost every $x \in \pi(K)$. Therefore almost all the fibers are strictly convex. $\square$

4.1.1. Puffed polytopes

In this section we introduce a particular class of convex bodies arising from polytopes. A known concept in the context of hyperbolic polynomials and hyperbolicity cones is that of the *derivative cone*; see [Ren06] or [San13]. Since we are dealing with compact objects, we will repeat the same construction in affine coordinates, i.e. for polytopes instead of polyhedral cones.

Let P be a full–dimensional polytope in $\mathbb{R}^N$, containing the origin, with d facets given by affine equations $l_1(x_1, \ldots, x_N) = a_1, \ldots, l_d(x_1, \ldots, x_N) = a_d$. Consider the polynomial

$$p(x_1, \ldots, x_N) = \prod_{i=1}^{d} (l_i(x_1, \ldots, x_N) - a_i). \tag{4.1.4}$$

Its zero locus is the algebraic boundary of P, i.e. the algebraic closure of the boundary, in the Zariski topology, as in [Sin15]. Consider the homogenization of p, that is $\tilde{p}(x_1, \ldots, x_N, w) = \prod_{i=1}^{d} (l_i(x_1, \ldots, x_N) - a_i w)$. It is the algebraic boundary of a polyhedral cone and it is hyperbolic with respect to the direction $(0, \ldots, 0, 1) \in \mathbb{R}^{N+1}$. Then for all $i < d$ the polynomial

$$\left(\frac{\partial^i}{\partial w^i} \tilde{p} \right) (x_1, \ldots, x_N, 1) \tag{4.1.5}$$

is the algebraic boundary of a convex set containing the origin, see [San13].

Definition 4.1.14. Let Z_i be the zero locus of (4.1.5) in $\mathbb{R}^N$. The *i-th puffed P* is the closure of the connected component of the origin in $\mathbb{R}^N \setminus Z_i$. We denote it by $\mathrm{puff}_i(P)$.

In particular the first puffed polytope is always a spectrahedron [San13]. As the name suggests, the puffed polytopes $\mathrm{puff}_i(P)$ are fat, inflated versions of the polytope P and in fact contain P. On the other hand, despite the definition involves a derivation, the operation of "taking the puffed" does not behave as a derivative. In particular $\mathrm{puff}_i(P) \neq \mathrm{puff}_1\left(\mathrm{puff}_{i-1}(P)\right)$ because for a convex body which is not a polytope this operation is not even defined, and it does not commute with the Minkowski sum, as explained in the next example.

Proposition 4.1.15. In general for polytopes P_1, P_2

$$\mathrm{puff}_1(P_1 + P_2) \neq \mathrm{puff}_1(P_1) + \mathrm{puff}_1(P_2).$$

Proof. We build a counterexample in dimension $N = 2$. Let us consider two squares $P_1 = \mathrm{conv}\{(\pm 1, \pm 1)\}$, $P_2 = \mathrm{conv}\{(0, \pm 1), (\pm 1, 0)\} \subset \mathbb{R}^2$. The first puffed square is a disc with radius half of the diagonal, so $\mathrm{puff}_1(P_1)$ has radius $\sqrt{2}$ and $\mathrm{puff}_1(P_2)$ has radius 1. Therefore $\mathrm{puff}_1(P_1) + \mathrm{puff}_1(P_2)$ is a disc centered at the origin of radius $1 + \sqrt{2}$. On the other hand $P_1 + P_2$ is an octagon. Its associated polynomial in (4.1.4) is

$$p(x, y) = ((x + y)^2 - 9)((x - y)^2 - 9)(x^2 - 4)(y^2 - 4).$$

Via the procedure explained above we obtain the boundary of this puffed octagon, as the zero locus of the following irreducible polynomial

$$2x^6 + 7x^4y^2 + 7x^2y^4 + 2y^6 - 88x^4 - 193x^2y^2 - 88y^4 + 918x^2 + 918y^2 - 2592.$$

This is a curve with three real connected comonents, shown in violet in Figure 4.2. Clearly the puffed octagon is not a circle, hence $\mathrm{puff}_1(P_1) + \mathrm{puff}_1(P_2) \neq \mathrm{puff}_1(P_1 + P_2)$. $\square$
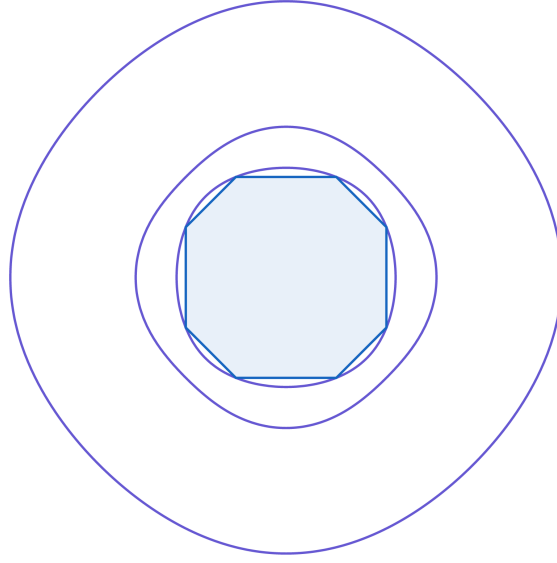
Figure 4.2: The octagon, in blue, and (the algebraic boundary of) its puffed octagon, in violet.

Strict convexity of the puffed polytopes. Our aim is to study the strict convexity of the fiber body of a puffed polytope. In order to do so, we shall at first say something more about the boundary structure of a puffed itself.

Lemma 4.1.16. Let $P \subset \mathbb{R}^N$ be a full–dimensional polytope. Then all faces F of P of dimension $k < N - i$, are contained in the boundary of $\mathrm{puff}_i(P)$.

Proof. Let F be a $k-$face of P; it is contained in the zero set of the polynomial (4.1.4). Moreover F arises as the intersection of at least $N - k$ facets (i.e. faces of dimension $N - 1$), thus its points are zeros of multiplicity at least $N - k$. Hence, if $N - k > i$ the face F is still in the zero set of (4.1.5), i.e. it belongs to the boundary of $\mathrm{puff}_i(P)$. □

The other direction is not always true: there may be k–faces of P, with $k \geq N - i$, whose points are zeros of (4.1.5) of multiplicity higher than i, and hence faces of $\mathrm{puff}_i(P)$. However there are two cases in which this is not possible.

Lemma 4.1.17. Let $P \subset \mathbb{R}^N$ be a full–dimensional polytope.

- $i = 1$: the flat faces in the boundary of $\mathrm{puff}_1(P)$ are exactly the faces of dimension $k < N - 1$;

- $i = 2$: the flat faces in the boundary of $\mathrm{puff}_2(P)$ are exactly the faces of dimension $k < N - 2$.

Proof. The first point is clear because the facets (faces of dimension $N - 1$) are the only zeroes of multiplicity one. The second point follows from the so called "diamond property" of polytopes [Zie12]. □

Remark 4.1.18. By [Ren06, Proposition 24] we can deduce that the flat faces of a puffed polytope must be faces of the polytope itself. The remaining points in the boundary of $\mathrm{puff}_i(P)$ are exposed points.

Using this result we can deduce conditions for the strict convexity of the fiber body of a puffed polytope.

Proposition 4.1.19 (Fiber 1st puffed polytope)**.** Let $P \subset \mathbb{R}^{n+m}$ be a full–dimensional polytope, $n \geq 1$, $m \geq 2$, and take any projection $\pi : \mathbb{R}^{n+m} \to \mathbb{R}^n$. The fiber puffed polytope $\Sigma_\pi \left(\mathrm{puff}_1 \left(P \right) \right)$ is strictly convex if and only if $m = 2$.

Proof. By Lemma 4.1.17, the flat faces in the boundary of $\mathrm{puff}_1 \left(P \right)$ are the faces of P of dimension $k < n + m - 1$. Suppose first that $m > 2$ and let F be a $(n + m - 2)$–face of P. Take a point p in the relative interior of F and let $x_p := \pi(p)$. Then the dimension of $F \cap \pi^{-1}(x_p)$ is at least $m - 2 \geq 1$; we can also assume without loss of generality that

$$1 \leq \dim \left(F \cap \pi^{-1}(x_p) \right) < n + m - 2. \tag{4.1.6}$$

Furthermore there is a whole neighborhood U of x_p such that condition (4.1.6) holds, so for every $x \in U$ the convex body $(\mathrm{puff}_1 \left(P \right))_x$ is not strictly convex. By Proposition 4.1.13 then $\Sigma_\pi \left(\mathrm{puff}_1 \left(P \right) \right)$ is not strictly convex. Suppose now that $m = 2$ and fix a flat face F of $\mathrm{puff}_1 \left(P \right)$. Its dimension is less or equal than n, so $(F \cap \pi^{-1}(x_p))$ is either one point or a face of positive dimension. In the latter case $\dim \pi(F) \leq n - 1$, i.e. it is a set of measure zero in $\pi \left(\mathrm{puff}_1 \left(P \right) \right)$. Because there are only finitely many flat faces, we can conclude that almost all the fibers are strictly convex and thus by Proposition 4.1.13, $\Sigma_\pi \left(\mathrm{puff}_1 \left(P \right) \right)$ is strictly convex. $\qquad \square$

A similar result holds for the second fiber puffed polytope, using Lemma 4.1.17.

Proposition 4.1.20 (Fiber 2nd puffed polytope)**.** Let $P \subset \mathbb{R}^{n+m}$ be a full–dimensional polytope, $n \geq 1$, $m \geq 2$, and take any projection $\pi : \mathbb{R}^{n+m} \to \mathbb{R}^n$. The fiber puffed polytope $\Sigma_\pi \left(\mathrm{puff}_2 \left(P \right) \right)$ is strictly convex if and only if $m \leq 3$, i.e. $m = 2$ or 3.

Proof. We can use the previous strategy again. If $m > 3$, there always exists a face of $\mathrm{puff}_2 \left(P \right)$ of dimension $n + m - 3$ whose non–empty intersection with fibers of π has dimension at least 1 and strictly less than $n + m - 3$. So in this case we get a non strictly convex fiber body. On the other hand, when $m = 2$ or 3 the intersection of the fibers and the flat faces has positive dimension only on a measure zero subset of $\mathbb{R}^n$, hence almost all the fibers are strictly convex and the thesis follows. $\qquad \square$

Can we generalize this result for the i-th puffed polytope? In general no, and the reason is precisely that a k-face may be contained in more than $(n + m - k)$ facets, when $k < n + m - 2$. The polytopes P for which this does not happen are called *simple polytopes*. Thus with the same proof as above we obtain the following.

Proposition 4.1.21 (Fiber i-th puffed simple polytope)**.** Let $P \subset \mathbb{R}^{n+m}$ be a full–dimensional simple polytope, $n \geq 1$, $m \geq 2$, and take any projection $\pi : \mathbb{R}^{n+m} \to \mathbb{R}^n$. The fiber puffed polytope $\Sigma_\pi \left(\mathrm{puff}_i \left(P \right) \right)$ is strictly convex if and only if $m \leq i + 1$.

In the case where P is not simple, one has to take into account the number of facets in which each face of dimension $k \geq n + m - i$ is contained, in order to understand if they are or not part of the boundary of $\mathrm{puff}_i \left(P \right)$.

A case study: the elliptope.   Take the tetrahedron $\mathcal{T}$ in $\mathbb{R}^3$ realized as

$$\mathrm{conv}\{(1, 1, 1), (1, -1, -1), (-1, 1, -1), (-1, -1, 1)\}.$$

(a)

(b)
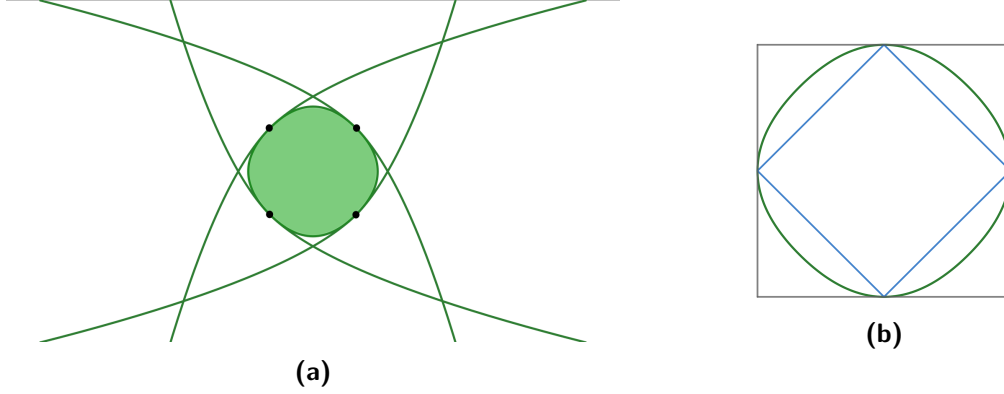
Figure 4.3: Left: the four green parabolas meet in the four black points on the boundary of the fiber elliptope, that lie on the diagonals $y = z$ and $y = -z$.
Right: sandwiched fiber bodies. The blue rhombus is the fiber tetrahedron $\Sigma_\pi \mathcal{T}$; the green convex body is the fiber elliptope $\Sigma_\pi \mathcal{E}$; the grey square is the fiber cube $\Sigma_\pi \left([-1, 1]^3 \right)$.

The first puffed tetrahedron (for the rest of the paragraph we will omit the word "first") is the semialgebraic convex body called *elliptope* which is the set of points $(x, y, z) \in [-1, 1]^3$ such that $x^2 + y^2 + z^2 - 2xyz \le 1$. Let π be the projection on the first coordinate: $\pi(x, y, z) = x$. The fibers of the elliptope at x for $x \in (-1, 1)$ are the ellipses defined by

$$\mathcal{E}_x = \left\{ (y, z) \mid \left(\frac{y - xz}{\sqrt{1 - x^2}} \right)^2 + z^2 \le 1 \right\}.$$

Introducing the matrix

$$M_x := \begin{pmatrix} \frac{1}{\sqrt{1-x^2}} & \frac{-x}{\sqrt{1-x^2}} \\ 0 & 1 \end{pmatrix}$$

it turns out that $\mathcal{E}_x = \{ (y, z) \mid \| M_x(y, z) \|^2 \le 1 \} = (M_x)^{-1} B^2$, where B^2 is the unit 2–disc. We obtain

$$h_{\mathcal{E}_x}(u, v) = h_{B^2} \left((M_x)^{-T}(u, v) \right) = \left\| (M_x)^{-T}(u, v) \right\| = \sqrt{u^2 + v^2 + 2xuv}.$$

By (4.1.2) we need to compute the integral of $h_{\mathcal{E}_x}$ between $x = -1$ and $x = 1$ to obtain the support function of the fiber body of the elliptope. We get

$$h_{\Sigma_\pi \mathcal{E}}(u, v) = \frac{1}{3uv} \left(|u + v|^3 - |u - v|^3 \right).$$

Hence the fiber body is semialgebraic and its algebraic boundary is the zero set of the four parabolas $3y^2 + 8z - 16$, $3y^2 - 8z - 16$, $8y + 3z^2 - 16$, $8y - 3z^2 + 16$, displayed in Figure 4.3a.

As anticipated in Proposition 4.1.19 the fiber elliptope is strictly convex. Notice that the elliptope is naturally sandwiched between two polytopes: the tetrahedron $\mathcal{T}$ and the cube $[-1, 1]^3$. Therefore, as a natural consequence of the definition, the same chain of inclusions works also for their fiber bodies:

$$\Sigma_\pi \mathcal{T} \subset \Sigma_\pi \mathcal{E} \subset \Sigma_\pi \left([-1, 1]^3 \right)$$

as shown in Figure 4.3b.

Remark 4.1.22. From this example it is clear that the operation of "taking the fiber body" does not commute with the operation of "taking the puffed polytope". In fact the puffed polytope of the blue square in Figure 4.3b is not the green convex body bounded by the four parabolas: it is the disc $y^2 + z^2 \leq 4$.

4.1.2. Curved convex bodies

In this section we are interested in the case where the boundary of the convex body K is highly regular. We prove Theorem 4.1.26 which is a formula to compute support function of the fiber body directly in terms of the support function of K, without having to compute those of the fibers.

Definition 4.1.23. We say that a convex body K is *curved* if its support function h_K is C^2 and the gradient ∇h_K restricted to the sphere is a C^1 diffeomorphism with the boundary of K.

In that case K is full–dimensional and its boundary is a C^2 hypersurface. Moreover we have the following.

Lemma 4.1.24. Let $K \subset \mathbb{R}^{n+m}$ be a curved convex body and let $v \in S^{n+m-1}$. Then the differential $\mathrm{d}_v \nabla h_K$ is a symmetric positive definite automorphism of $v^\perp$.

Proof. This is proved in [Sch13, p.116], where curved convex bodies are said to be "of class C_+^2" and $\mathrm{d}_v \nabla h_K$ is denoted by $\overline{W}_v$. □

The following gives an expression for the face of the fiber body. This is to be compared with the case of polytopes which is given in [EK08, Lemma 11].

Lemma 4.1.25. If K is a curved convex body and $u \in W$ with $\|u\| = 1$, then

$$\nabla h_{\Sigma_\pi K}(u) = \int_V \nabla h_K(u + \xi) \cdot J_{\psi_u}(\xi) \, \mathrm{d}\xi$$

where $\psi_u : V \to V$ is given by $\psi_u(\xi) = (\pi \circ \nabla h_K)(u + \xi)$ and $J_{\psi_u}(\xi)$ denotes its Jacobian (i.e. the determinant of its differential) at the point ξ.

Proof. From (4.1.3) we have that $\nabla h_{\Sigma_\pi K}(u) = \int_{\pi(K)} \gamma_u(x) \mathrm{d}x$, where $\gamma_u(x) = \nabla h_{K_x}(u)$. Assume that $x = \psi_u(\xi)$ is a change of variables. We get $\gamma_u(x) = (\gamma_u \circ \pi \circ \nabla h_K)(u + \xi) = \nabla h_K(u + \xi)$ and the result follows.

It remains to prove that it is indeed a change of variables. Note that $\nabla h_K(u + \xi) = \nabla h_K(v)$ where $v = \frac{u+\xi}{\|u+\xi\|} \in S^{n+m-1}$. The differential of the map $\xi \mapsto v$ maps V to $(V + \mathbb{R}u) \cap v^\perp$. Moreover ∇h_K restricted to the sphere is a C^1 diffeomorphism by assumption. Thus it only remains to prove that its differential $\mathrm{d}_v \nabla h_K$ sends $(V + \mathbb{R}u) \cap v^\perp$ to a subspace that does not intersect $\ker\left(\pi|_{v^\perp}\right)$. To see this, note that $\ker\left(\pi|_{v^\perp}\right)^\perp = (V + \mathbb{R}u) \cap v^\perp$. Moreover, by the previous lemma, we have that $\langle w, \mathrm{d}_v \nabla h_K \cdot w \rangle = 0$ if and only if $w = 0$. Thus if $w \in \ker\left(\pi|_{v^\perp}\right)^\perp$ and $w \neq 0$, then $\pi\left(\mathrm{d}_v \nabla h_K \cdot w\right) \neq 0$. Putting everything together, this proves that $\mathrm{d}_\xi \psi_u$ has no kernel which is what we wanted. □

As a direct consequence we derive a formula for the support function.

Theorem 4.1.26. Let $K \subset \mathbb{R}^{n+m}$ be a curved convex body. Then the support function of $\Sigma_\pi K$ is for all $u \in W$

$$h_{\Sigma_\pi K}(u) = \int_V \langle u, \nabla h_K(u + \xi) \rangle \cdot J_{\psi_u}(\xi) \, \mathrm{d}\xi \tag{4.1.7}$$

where $\psi_u : V \to V$ is given by $\psi_u(\xi) = (\pi \circ \nabla h_K)(u + \xi)$ and $J_{\psi_u}(\xi)$ denotes its Jacobian at the point ξ.

Proof. Apply the previous lemma to $h_{\Sigma_\pi K}(u) = \langle u, \nabla h_{\Sigma_\pi K}(u) \rangle$. $\square$

Assume that the support function h_K is *algebraic*, i.e. it is a root of some polynomial equation. Then the integrand in Lemma 4.1.25 and in Theorem 4.1.26 is also algebraic. Indeed it is simply $\nabla h_K(u + \xi)$ times the Jacobian of ψ_u which is a composition of algebraic functions. We can generalize this concept in the direction of the so called D–modules [SS19]. One can define what it means for a D–ideal of the Weyl algebra D to be *SatStu:DModulesHolonomicFunctions*. Then a function is holonomic if its annihilator, a D–ideal, is holonomic. Intuitively this means that such function satisfies a system of linear homogeneous (in the function and its derivatives) differential equations with polynomial coefficients, plus a suitable dimension condition. It can be proved that holonomicity is a generalization of algebraicity. We say that a convex body K is *holonomic* if its support function h_K is holonomic. In this setting, the fiber body satisfies the following property.

Corollary 4.1.27. If K is a curved holonomic convex body, then its fiber body is again holonomic.

Proof. We prove that the integrand in Theorem 4.1.26 is a holonomic function of u and ξ. Then the result follows from the fact that the integral of a holonomic function is holonomic [SS19, Proposition 2.11]. If h_K is holonomic then $\nabla h_K(u + \xi)$ is a holonomic function of u and ξ, as well as its scalar product with u. It remains to prove that the Jacobian of ψ_u is holonomic. But ψ_u is the projection of a holonomic function and thus holonomic, so the result follows. $\square$

A case study: Schneider's polynomial body. In [Sch13, p.203] Schneider exhibits an example of a one parameter family of semialgebraic centrally symmetric convex bodies that are not zonoids (see Section 4.1.3 for a definition of zonoids). Their support function is polynomial when restricted to the sphere. We will show how in that case Theorem 4.1.26 makes the computation of the fiber body relatively easy.

Definition 4.1.28. Schneider's polynomial body is the convex body $\mathcal{S}_\alpha \in \mathcal{K}(\mathbb{R}^3)$ whose support function is given by (see [Sch13, p.203])

$$h_{\mathcal{S}_\alpha}(u) = \|u\| \left(1 + \frac{\alpha}{2} \left(\frac{3(u_3)^2}{\|u\|^2} - 1 \right) \right)$$
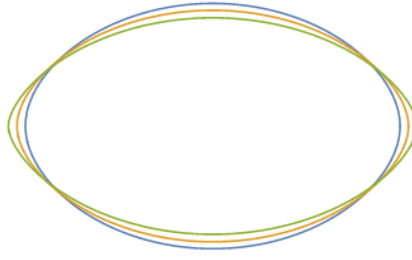
for $\alpha \in [-8/20, -5/20]$.

Let $\pi := \langle e_1, \cdot \rangle : \mathbb{R} \oplus \mathbb{R}^2 \to \mathbb{R}$ be the projection onto the first coordinate. We want to apply Theorem 4.1.26 to compute the support function of $\Sigma_\pi \mathcal{S}_\alpha$. For the gradient we obtain:

$$\nabla h_{\mathcal{S}_\alpha}(u) = \frac{1}{2\|u\|^3} \begin{pmatrix} -u_1 \left((u_1)^2(\alpha - 2) + (u_2)^2(\alpha - 2) + 2(u_3)^2(2\alpha - 1) \right) \\ -u_2 \left((u_1)^2(\alpha - 2) + (u_2)^2(\alpha - 2) + 2(u_3)^2(2\alpha - 1) \right) \\ \frac{u_3}{\|u\|^2} \left((u_1)^2(5\alpha + 2) + (u_2)^2(5\alpha + 2) + 2(u_3)^2(2\alpha + 1) \right) \end{pmatrix}.$$

For $u = (0, u_2, u_3)$, the Jacobian is $J_{\psi_u}(t) = \frac{\mathrm{d}}{\mathrm{d}t} (\pi \circ \nabla h_{\mathcal{S}_\alpha}(t, u_2, u_3))$, which gives

$$J_{\psi_u}(t) = \frac{t^2 (-(u_2)^2(\alpha - 2) + (u_3)^2(5\alpha + 2)) - \|u\|^2((u_2)^2(\alpha - 2) + 2(u_3)^2(2\alpha - 1))}{2(t^2 + \|u\|^2)^{\frac{5}{2}}}.$$

Figure 4.4: Fiber body of Schneider's polynomial body for $\alpha = -i/20$ with $i = 5, 6$ and 7

Substituting in (4.1.7), we integrate $\langle u, \nabla h_{\mathcal{S}_\alpha}(t, u_2, u_3) \rangle J_{\psi_u}(t)$ and get the support function of the fiber body (see Figure 4.4) which is again polynomial:

$$h_{\Sigma_\pi \mathcal{S}_\alpha}(u) = \frac{\pi}{64\|u\|^3} \left(8(\alpha - 2)(u_2)^4 - 8(\alpha^2 + 2\alpha - 8)(u_2)^2(u_3)^2 + (-25\alpha^2 + 16\alpha + 32)(u_3)^4 \right).$$

4.1.3. Zonoids

In this section, we focus on the class of *zonoids*. Let us first recall some definitions and introduce some notation. For more details we refer to [Sch13, Section 3.5].

We will use the following notation for centered segments: for any $x \in \mathbb{R}^{n+m}$ we write

$$\underline{x} := \frac{1}{2} [-x, x]. \tag{4.1.8}$$

Definition 4.1.29. A convex body $K \in \mathcal{K}(\mathbb{R}^{n+m})$ is called a *zonotope* if there exist $x_1, \ldots x_N \in \mathbb{R}^{n+m}$ such that, with the notation introduced above, $K = \underline{x_1} + \cdots + \underline{x_N}$. A *zonoid* is a limit (in the Hausdorff distance) of zonotopes. The space of zonoids of $\mathbb{R}^{n+m}$ will be denoted by $\mathscr{Z}_0(\mathbb{R}^{n+m})$.

Remark 4.1.30. It follows immediately from the definition that all zonoids are centrally symmetric centered in the origin, i.e. if $K \in \mathscr{Z}_0(\mathbb{R}^{n+m})$ then $(-1)K = K$. In general the definition of zonoids may also include translations of such bodies. The elements of $\mathscr{Z}_0(\mathbb{R}^{n+m})$ are then called *centered* zonoids. For simplicity here we chose to omit the term "centered".

We introduce the approach of Vitale in [Vit91] using random vectors. The following is [Vit91, Theorem 3.1] rewritten in our context.

Proposition 4.1.31. A convex body $K \in \mathcal{K}(\mathbb{R}^{n+m})$ is a zonoid if and only if there is a random vector $X \in \mathbb{R}^{n+m}$ with $\mathbb{E}\|X\| < \infty$ such that for all $u \in \mathbb{R}^{n+m}$

$$h_K(u) = \frac{1}{2}\mathbb{E}\left| \langle u, X \rangle \right|. \tag{4.1.9}$$

We call such a zonoid the *Vitale zonoid* associated to the random vector X, and denote it by $K_0(X)$.

The fiber body of a zonoid. We now show that the fiber body of a zonoid is a zonoid and give a formula to compute it in Theorem 4.1.37. Let us first introduce some of the tools used by Esterov in [Est08].

Definition 4.1.32. For any $u \in W$ define $T_u := Id_V \oplus \langle u, \cdot \rangle : V \oplus W \to V \oplus \mathbb{R}$.

Definition 4.1.33. Let $C \in \mathcal{K}(V \oplus \mathbb{R})$. The *shadow volume* $V_+(C)$ of C is defined to be the integral of the maximal function on $\pi(C) \subset V$ such that its graph is contained in C, i.e.

$$V_+(C) = \int_{\pi(C)} \varphi(x)\mathrm{d}x,$$

where $\varphi(x) = \sup\{t \mid (x,t) \in C\}$. In particular if $(-1)C = C$, then the shadow volume is $V_+(C) = \frac{1}{2}\mathrm{vol}_{n+1}(C)$.

The *shadow volume* can then be used to express the support function of the fiber body.

Lemma 4.1.34. For $u \in W$ and $K \in \mathcal{K}(\mathbb{R}^{n+m})$, we have

$$h_{\Sigma_\pi K}(u) = V_+(T_u(K)).$$

In particular if $(-1)K = K$,

$$h_{\Sigma_\pi K}(u) = \frac{1}{2}\mathrm{vol}_{n+1}(T_u(K)). \tag{4.1.10}$$

Proof. We also denote by $\pi : V \oplus \mathbb{R} \to V$ the projection onto V. The shadow volume is the integral on $\pi(T_u(K)) = \pi(K)$ of the function $\varphi(x) = \sup\{t \mid (x,t) \in T_u(K)\} = \sup\{\langle u,y \rangle \mid (x,y) \in K\} = h_{K_x}(u)$. Thus the result follows from Proposition 4.1.6. $\qquad \square$

Remark 4.1.35. Note that if $m = 2$ then T_u is the projection onto the hyperplane spanned by V and u. In that case (4.1.10) is the formula for the support function of the Π–body of K at Ju, where J is a rotation by $\pi/2$ in W. Thus in that case, $\Sigma_\pi K$ is the projection of ΠK onto W rotated by $\pi/2$.

We will show that the mixed fiber body of zonoids comes from a multilinear map defined directly on the vector spaces.

Definition 4.1.36. We define the following (completely skew-symmetric) multilinear map:

$$F_\pi : (V \oplus W)^{n+1} \to W$$

$$(x_1 + y_1, \ldots, x_{n+1} + y_{n+1}) \mapsto \frac{1}{(n+1)!}\sum_{i=1}^{n+1}(-1)^{n+1-i}(x_1 \wedge \cdots \wedge \widehat{x_i} \wedge \cdots \wedge x_{n+1})y_i$$

where $x_1 \wedge \cdots \wedge \widehat{x_i} \wedge \cdots \wedge x_{n+1}$ denotes the determinant of the chosen vectors omitting x_i.

We are now able to prove the main result of this section, here stated in the language of the Vitale zonoids introduced in Proposition 4.1.31.

Theorem 4.1.37. The fiber body of a zonoid is the zonoid. Moreover, if $X \in \mathbb{R}^{n+m}$ is a random vector such that $\mathbb{E}\|X\| < \infty$ and $K := K_0(X)$ is the associated Vitale zonoid, then

$$\Sigma_\pi K = K_0(F_\pi(X_1, \ldots, X_{n+1}))$$

where $X_1, \ldots, X_{n+1} \in \mathbb{R}^{n+m}$ are i.i.d. copies of X. In other words, the support function of the fiber body $\Sigma_\pi K$ is given for all $u \in W$ by

$$h_{\Sigma_\pi K}(u) = \frac{1}{2}\mathbb{E}|\langle u, Y \rangle| \tag{4.1.11}$$

where $Y \in W$ is the random vector defined by $Y := F_\pi(X_1, \ldots, X_{n+1})$.

Proof. Suppose that $K = K_0(X)$ and let $u \in W$. Note that by (4.1.9) and Proposition 2.1.19–(*ii*), $T_u(K) = K_0(T_u(X_1))$. Thus by (4.1.10) and [Vit91, Theorem 3.2] we get

$$h_{\Sigma_\pi K}(u) = \tfrac{1}{2}\operatorname{vol}(K_0(T_u(X))) = \tfrac{1}{2}\tfrac{1}{(n+1)!}\mathbb{E}|T_u(X_1) \wedge \cdots \wedge T_u(X_{n+1})| \qquad (4.1.12)$$

where $X_1, \ldots, X_{n+1} \in \mathbb{R}^{n+m}$ are iid copies of X.

Now let us write $X_i := \alpha_i + \beta_i$ with $\alpha_i \in V$ and $\beta_i \in W$. Then

$$|T_u(X_1) \wedge \cdots \wedge T_u(X_{n+1})| = |(\alpha_1 + \langle u, \beta_1 \rangle) \wedge \cdots \wedge (\alpha_{n+1} + \langle u, \beta_{n+1} \rangle)|$$

$$= \left| \sum_{i=1}^{n+1} (-1)^{n+1-i}(\alpha_1 \wedge \cdots \wedge \widehat{\alpha_i} \wedge \cdots \wedge \alpha_{n+1})\langle u, \beta_i \rangle \right|$$

$$= |\langle u, (n+1)! F_\pi(\alpha_1 + \beta_1, \ldots, \alpha_{n+1} + \beta_{n+1}) \rangle|.$$

Reintroducing this in (4.1.12) we obtain (4.1.11).

$\square$

This allows to generalize [BS92, Theorem 4.1] for all zonotopes.

Corollary 4.1.38. For all $z_1, \ldots, z_N \in \mathbb{R}^{n+m}$, the fiber body of the zonotope $\sum_{i=1}^{N} \underline{z_i}$ is the zonotope given by

$$\Sigma_\pi \left(\sum_{i=1}^{N} \underline{z_i} \right) = (n+1)! \sum_{1 \le i_1 < \cdots < i_{n+1} \le N} \underline{F_\pi(z_{i_1}, \ldots, z_{i_{n+1}})}$$

where we used the notation of (4.1.8), writing $\underline{x}$ for the segment $[-x/2, x/2]$.

Proof. We apply Theorem 4.1.37 to the discrete random vector X, that is equal to $N z_i$ with probability $1/N$ for all $i = 1, \ldots, N$. In that case one can check from (4.1.9) that the Vitale zonoid $K_0(X)$ is precisely the zonotope $\sum_{i=1}^{N} \underline{z_i}$, and the result follows from (4.1.11). $\square$

Esterov shows in [Est08] that the map $\Sigma_\pi : \mathcal{K}(\mathbb{R}^{n+m}) \to \mathcal{K}(W)$ comes from another map, which is (Minkowski) multilinear in each variable: the so called *mixed fiber body*. The following is [Est08, Theorem 1.2].

Proposition 4.1.39. There is a unique continuous multilinear map

$$\mathrm{M}\Sigma_\pi : \left(\mathcal{K}(\mathbb{R}^{n+m}) \right)^{n+1} \to \mathcal{K}(W)$$

such that for all $K \in \mathcal{K}(\mathbb{R}^{n+m})$, $\mathrm{M}\Sigma_\pi(K, \ldots, K) = \Sigma_\pi(K)$.

Once its existence is proved, one can see that the mixed fiber body $\mathrm{M}\Sigma_\pi(K_1, \ldots, K_{n+1})$ is the coefficient of $t_1 \cdot \ldots \cdot t_{n+1}$, divided by $(n+1)!$, in the expansion of $\Sigma_\pi(t_1 K_1 + \cdots + t_{n+1} K_{n+1})$. Using this *polarization formula*, one can deduce from Theorem 4.1.37 a similar statement for the mixed fiber body of zonoids.

Proposition 4.1.40. The mixed fiber body of zonoids is a zonoid. Moreover, if $X_1, \ldots, X_{n+1} \in \mathbb{R}^{n+m}$ are independent (not necessarily identically distributed) random vectors such that $\mathbb{E}\|X_i\|$ is finite, and $K_i := K_0(X_i)$ are the associated Vitale zonoids, then

$$\mathrm{M}\Sigma_\pi(K_1, \ldots, K_{n+1}) = K_0(F_\pi(X_1, \ldots, X_{n+1})).$$

Proof. Let us show the case of $n + 1 = 2$ variables. The general case is done in a similar way. Let $\tilde{X} := t_1 \alpha 2 X_1 + t_2 (1 - \alpha) 2 X_2$ where α is a Bernoulli random variable of parameter $1/2$ independent of X_1 and X_2. Using (4.1.9), one can check that $K_0(\tilde{X}) = t_1 K_1 + t_2 K_2$. Now let Y_1 (respectively Y_2) be an i.i.d. copy of X_1 (respectively X_2) independent of all the other variables. Define $\tilde{Y} := t_1 \beta 2 Y_1 + t_2 (1 - \beta) 2 Y_2$ where β is a Bernoulli random variable of parameter $1/2$ independent of all the other variables. By Theorem 4.1.37 we have that $\Sigma_\pi(t_1 K_1 + t_2 K_2) = K_0(F_\pi(\tilde{X}, \tilde{Y}))$. By (4.1.9), using the independence assumptions, it can be deduced that for all $t_1, t_2 \geq 0$

$$h_{K_0(F_\pi(\tilde{X}, \tilde{Y}))} = t_1^2 h_{\Sigma_\pi K_1} + t_2^2 h_{\Sigma_\pi K_2} + t_1 t_2 (h_{K_0(F_\pi(X_1, Y_2))} + h_{K_0(F_\pi(X_2, Y_1))}).$$

The claim follows from the fact that $K_0(F_\pi(X_1, Y_2)) = K_0(F_\pi(X_2, Y_1)) = K_0(F_\pi(X_1, X_2))$. $\qquad\square$

Discotopes.   In this section, we investigate the fiber bodies of finite Minkowski sums of discs in $\mathbb{R}^3$, called *discotopes*. They also appear in the literature, see [AS16] for example. Discotopes are zonoids (because discs are zonoids see Lemma 4.1.42 below) that are not polytopes nor curved (see Section 4.1.2) but still have simple combinatorial properties and a simple support function. We will see how in this case formula (4.1.11) can be useful to compute the fiber body.

Definition 4.1.41. Let $v \in \mathbb{R}^3$, we denote by D_v the disc in $v^\perp$ centered at 0 of radius $\|v\|$.

Lemma 4.1.42. Discs are zonoids. If a, b is an orthonormal basis of $v^\perp$, we define the random vector $\sigma(\theta) := \|v\|(\cos(\theta)a + \sin(\theta)b)$ with $\theta \in [0, 2\pi]$ uniformly distributed. Then we have

$$D_v = \pi \cdot K_0(\sigma(\theta)) \tag{4.1.13}$$

where we recall the definition of the Vitale Zonoid associated to a random vector in Proposition 4.1.31. In other words we have:

$$h_{D_v}(u) = \|v\|\sqrt{\langle u, a \rangle^2 + \langle u, b \rangle^2} = \frac{\pi}{2} \mathbb{E}|\langle u, \sigma(\theta) \rangle|. \tag{4.1.14}$$

Proof. Consider the zonoid $K_0(\sigma(\theta))$. We will prove that it is a disc contained in $v^\perp$ centered at 0 of radius $\|v\|/\pi$.

First of all, since $\sigma(\theta) \in v^\perp$ almost surely, we have $h_{K_0(\sigma(\theta))}(\pm v) = 0$. Thus $K_0(\sigma(\theta))$ is contained in the plane $v^\perp$. Moreover, let $O(v^\perp)$ denote the stabilizer of v in the orthogonal group $O(3)$. The zonoid $K_0(\sigma(\theta))$ is invariant under the action of $O(v^\perp)$ thus it is a disc centered at 0. To compute its radius it is enough to compute the support function at one point: $h_{K_0(\sigma(\theta))}(a_1) = \|v\| \cdot \mathbb{E}|\cos(\theta)| = \|v\|/\pi$ and this concludes the proof. $\qquad\square$

Remark 4.1.43. Note that the law of the random vector $\sigma(\theta)$ does not depend on the choice of the orthonormal basis a, b. It only depends on the line spanned by v and the norm $\|v\|$.

Definition 4.1.44. A convex body $K \subset \mathbb{R}^3$ is called a *discotope* if it can be expressed as a finite Minkowski sum of discs, i.e. if there exist $v_1, \ldots, v_N \in \mathbb{R}^3$, such that $K = D_{v_1} + \cdots + D_{v_N}$. In particular discotopes are zonoids. Moreover we can and will assume without loss of generality that

$$\frac{v_i}{\|v_i\|} \neq \pm \frac{v_j}{\|v_j\|} \qquad \text{for } i \neq j.$$

What is the shape of a discotope? In order to answer this question we are going to study the boundary structure of such a convex body, when $N \geq 2$.

Lemma 4.1.45. Consider the discotope $K = D_{v_1} + \ldots + D_{v_N}$, fix $q \in \partial(D_{v_2} + \ldots + D_{v_N})$ and take the Minkowski sum $D_{v_1} + \{q\}$. Then such disc is part of the boundary of the discotope if and only if

$$\langle q, v_1 \rangle = \pm \max \left\{ \langle \tilde{q}, v_1 \rangle \mid \tilde{q} \in D_{v_2} + \ldots + D_{v_N} \right\}. \tag{4.1.15}$$

Proof. We do the proof for $N = 2$; the general case is then given by a straightforward induction.

Let $r : S^2 \to \mathbb{R}_{\geq 0}$ be the radial function of the discotope, namely $r(x) := \max \{\lambda \geq 0 \mid \lambda x \in K\}$. A point $x \in \partial K$ if and only if $r\left(\frac{x}{\|x\|}\right) = \|x\|$. So we claim that for all $p \in D_{v_1}$

$$r\left(\frac{p+q}{\|p+q\|}\right) = \|p+q\|$$

where $q \in D_{v_2}$ satisfies $\langle q, v_1 \rangle = \pm \max \{\langle \tilde{q}, v_1 \rangle \mid \tilde{q} \in D_{v_2}\}$. Assume first that q realizes the maximum. Let $r\left(\frac{p+q}{\|p+q\|}\right) = \lambda$. Then we have:

$$\lambda \left(\frac{p+q}{\|p+q\|}\right) = p' + q' \in \partial K$$

for some $p' \in D_{v_1}$ and $q' \in D_{v_2}$. By taking the scalar product with v_1 we get:

$$\frac{\lambda}{\|p+q\|} \langle q, v_1 \rangle = \langle q', v_1 \rangle \leq \langle q, v_1 \rangle$$

therefore $\lambda \leq \|p+q\|$. Since $p + q$ is a point of K, $\lambda \geq \|p+q\|$ and the thesis follows. The other case where q realizes the minimum is analogous. $\square$

Since we assumed that all the v_i are non colinear, for every i there are exactly two q_i that satisfy (4.1.15) that we will denote by q_i^+ and q_i^- respectively. Lemma 4.1.45 then says that in the boundary of the discotope there are exactly $2N$ discs, namely

$$D_{v_1} + \{q_1^+\}, \ D_{v_1} + \{q_1^-\}, \ \ldots, \ D_{v_N} + \{q_N^+\}, \ D_{v_N} + \{q_N^-\}.$$

The rest of the boundary of the discotope is the open surface $\mathcal{S} := \partial K \setminus \cup_{i=1}^{N} (D_{v_i} + \{q_i^{\pm}\})$ made of exposed points. Moreover we show in the next proposition that $\mathcal{S}$ has either one or two connected components.

Proposition 4.1.46. Consider the discotope $K = D_{v_1} + \ldots + D_{v_N}$, then $\mathcal{S}$ has two connected components if and only if $v_1, \ldots, v_N$ lie all in the same plane. Otherwise it is connected and no two discs intersect.

Proof. Assume first that $v_1, \ldots, v_N \in H$ where without loss of generality H is the hyperplane defined by $\{z = 0\}$, then we claim that all the discs in ∂K meet on H in a very precise configuration. Trivially the Minkowski sum $(D_{v_1} \cap H) + \ldots + (D_{v_N} \cap H)$ is contained in $K \cap H$. On the other hand let $p \in K \cap H$, then

$$p = (\alpha_1, \beta_1, \gamma_1) + \ldots + (\alpha_N, \beta_N, \gamma_N)$$

where $(\alpha_i, \beta_i, \gamma_i) \in D_{v_i}$ and $\sum \gamma_i = 0$. But because $v_i \in H$, then also $(\alpha_i, \beta_i, 0) \in D_{v_i}$ and so we can write p as

$$p = (\alpha_1, \beta_1, 0) + \ldots + (\alpha_N, \beta_N, 0)$$

hence $p \in (D_{v_1} \cap H) + \ldots + (D_{v_N} \cap H)$. This implies that $K \cap H$ is a 2–dimensional zonotope with $2N$ edges, as in Figure **??**; its vertices are exactly the points of intersection of the discs in the boundary. Hence the boundary discs divide $\mathcal{S}$ in exactly 2 connected components.

For the vice versa notice that if there are two connected components, then at least two boundary discs must intersect. Without loss of generality assume that there is an intersection point p between a copy of D_{v_1} and a copy of D_{v_2} and consider the plane $H = \mathrm{span}(v_1, v_2)$. Let $\pi(K)$ be the projection of the discotope on H; clearly $\pi(p) \in \partial\pi(K)$ is a vertex. Then for $u \in S^1 \hookrightarrow H$

$$h_{\pi(K)}(u) = h_{D_{v_1}}(u) + \ldots + h_{D_{v_N}}(u)$$

$$\overset{(4.1.14)}{=} \sum_{i=1}^{N} \|v_i\| \sqrt{\langle u, a_i \rangle^2 + \langle u, b_i \rangle^2}$$

$$= \sum_{i=1}^{N} \|v_i\| \sqrt{\langle u, \pi(a_i) \rangle^2 + \langle u, \pi(b_i) \rangle^2}$$

where $\{\frac{v_i}{\|v_i\|}, a_i, b_i\}$ is an orthonormal basis for every i. There are two possibilities now: either $\pi(a_i)$ and $\pi(b_i)$ are linearly independent, or they are linearly dependent and possibly zero. The latter case corresponds to discs such that $v_i \in H$, and the summand above becomes linear. So, up to relabeling, we can rewrite the support function splitting these cases:

$$h_{\pi(K)}(u) = \sum_{i=1}^{k} |\langle u, \alpha_i \rangle| + \sum_{j=k+1}^{N} \|v_j\| \sqrt{\langle u, \pi(a_j) \rangle^2 + \langle u, \pi(b_j) \rangle^2}$$

for some $\alpha_i \in \mathbb{R}$ and $2 \le k \le N$. Therefore $\pi(K)$ is the Minkowski sum of k line segments and $N - k$ ellipses. The boundary contains a vertex if and only if there are no ellipses in the sum, hence $k = N$ i.e. $v_i \in H$ for every i. $\square$

Remark 4.1.47. The previous result can be interpreted with the notion of *patches*. These geometric objects have been first introduced in [CKLS19] and allow to subdivide the boundary of a convex body. Accordingly to their definition, in the discotope we find $2N$ 2–patches, corresponding to the boundary discs, and either one ore two 0–patches when $\mathcal{S}$ has one or two connected components respectively. Recently Plaumann, Sinn and Wesner [PSW21] refined the definition of patches for a semialgebraic convex body. In this setting it is more subtle to count the number of patches of our discotopes, because this requires the knowledge of the number of irreducible components of $\mathcal{S}$.

A case study: the dice.

Definition 4.1.48. Let e_1, e_2, e_3 be the standard basis of $\mathbb{R}^3$ and let $D_i := D_{e_i}$. We define the *dice* to be the discotope $\mathscr{D} := D_1 + D_2 + D_3$. See Figure 4.5a.

The boundary of the dice consists of 6 two–dimensional discs of radius 1, lying in the center of the facets of the cube $[-2, 2]^3$, and a connected surface. The latter is the zero locus of the polynomial of degree 24:

$$\varphi(x, y, z) = x^{24} + 4x^{22}y^2 + 2x^{20}y^4 + \ldots + 728z^4 - 160x^2 - 160y^2 - 160z^2 + 16$$

which is too long to fit in a page (it is made of $91 + 78 + 66 + 55 + 45 + 36 + 28 + 21 + 15 + 10 + 6 + 3 + 1 = 455$ monomials, here distinguished by their degree).

Consider the projection $\pi := \langle e_1, \cdot \rangle : \mathbb{R} \oplus \mathbb{R}^2 \to \mathbb{R}$. Even in this simple example the fibers of the dice under this projection can be tricky to describe. However using the formula for zonoids one can compute explicitly the fiber body (see Figure 4.5b).

(a)

(b)
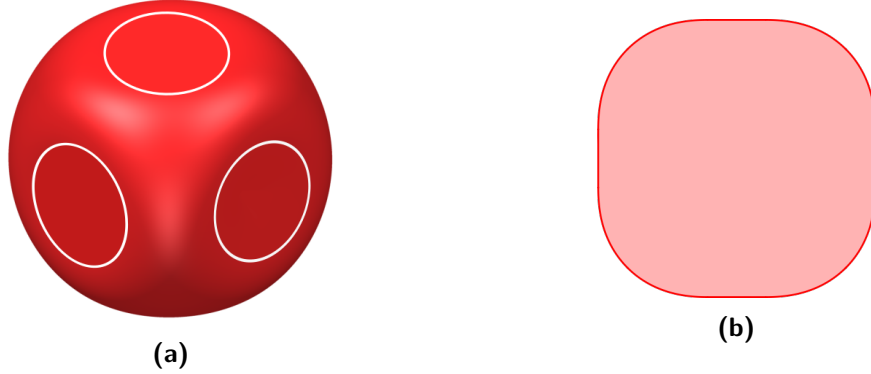
Figure 4.5: Left: the dice. Right: its fiber body.

Proposition 4.1.49. With respect to this projection π, the fiber body of $\mathscr{D}$ is

$$\Sigma_\pi(\mathscr{D}) = D_1 + \frac{\pi}{4}\left(\underline{e_2} + \underline{e_3}\right) + \frac{1}{2}\Lambda$$

where Λ is the convex body whose support function is given by

$$h_\Lambda(u_2, u_3) = \frac{1}{2}\int_0^\pi \sqrt{\cos(\theta)^2\,(u_2)^2 + \sin(\theta)^2\,(u_3)^2}\ \mathrm{d}\theta.$$

and where we recall the notation (4.1.8) for segments.

Proof. First of all let us note that by expanding the mixed fiber body $\mathrm{M}\Sigma_\pi(\mathscr{D}, \mathscr{D})$ we have

$$\Sigma_\pi(\mathscr{D}) = \Sigma_\pi(D_1) + \Sigma_\pi(D_2) + \Sigma_\pi(D_3) + 2\left(\mathrm{M}\Sigma_\pi(D_1, D_2) + \mathrm{M}\Sigma_\pi(D_1, D_3) + \mathrm{M}\Sigma_\pi(D_2, D_3)\right).$$

Now let $\sigma_1(\theta) := (0, \cos(\theta), \sin(\theta))$, $\sigma_2(\theta) := (\cos(\theta), 0, \sin(\theta))$ and $\sigma_3(\theta) := (\cos(\theta), \sin(\theta), 0)$ in such a way that $h_{D_i}(u) = \frac{\pi}{2}\mathbb{E}|\langle u, \sigma_i(\theta)\rangle|$.

We then want to use Theorem 4.1.37 and Proposition 4.1.40 to compute all the summands of the expansion of $\Sigma_\pi(\mathscr{D})$. Using (4.1.13) we have that $\mathrm{M}\Sigma_\pi(D_i, D_j) = \pi^2 K_0(F_\pi(\sigma_i(\theta), \sigma_j(\phi))$ with $\theta, \phi \in S^1$ uniform and independent. In our case, $F_\pi(x, y) = (x_1 y_2 - y_1 x_2, x_1 y_3 - y_1 x_3)/2$. We obtain

$$F_\pi(\sigma_1(\theta), \sigma_1(\phi)) = 0, \quad F_\pi(\sigma_2(\theta), \sigma_2(\phi)) = \frac{1}{2}(0, \sin(\phi - \theta)),$$

$$F_\pi(\sigma_3(\theta), \sigma_3(\phi)) = \frac{1}{2}(\sin(\phi - \theta), 0), \quad F_\pi(\sigma_1(\theta), \sigma_2(\phi)) = \frac{-\cos(\phi)}{2}(\cos(\theta), \sin(\theta)),$$

$$F_\pi(\sigma_1(\theta), \sigma_3(\phi)) = \frac{-\cos(\phi)}{2}(\cos(\theta), \sin(\theta)), \quad F_\pi(\sigma_2(\theta), \sigma_3(\phi)) = \frac{1}{2}(\cos(\theta)\sin(\phi), \sin(\theta)\cos(\phi)).$$

Computing the support function $h_{\pi^2 K_0(F_\pi(\sigma_i(\theta), \sigma_j(\phi)))} = (\pi^2/2)\mathbb{E}|\langle u, F_\pi(\sigma_i(\theta), \sigma_j(\phi))\rangle|$ and using that $\mathbb{E}|\cos(\phi)| = 2/\pi$, we get

$$\Sigma_\pi(D_1) = 0; \quad \Sigma_\pi(D_2) = \frac{\pi}{4}\ \underline{e_2}; \quad \Sigma_\pi(D_3) = \frac{\pi}{4}\ \underline{e_3};$$

$$\mathrm{M}\Sigma_\pi(D_1, D_2) = \mathrm{M}\Sigma_\pi(D_1, D_3) = \frac{1}{4}D_1$$

It only remains to compute $M\Sigma_\pi(D_2, D_3)$. We have

$$h_{M\Sigma_\pi(D_2,D_3)}(u) = \frac{1}{2}\left(\frac{\pi}{2}\right)^2 \mathbb{E}|\langle u, F_\pi(\sigma_2(\theta), \sigma_3(\phi))\rangle| = \frac{\pi^2}{16}\mathbb{E}|u_2\cos(\theta)\sin(\phi)+u_3\sin(\theta)\cos(\phi)|.$$

We use then the independence of θ and ϕ and (4.1.14) to find

$$h_{M\Sigma_\pi(D_2,D_3)}(u) = \frac{\pi}{8}\mathbb{E}\sqrt{\cos(\theta)^2\,(u_2)^2 + \sin(\theta)^2\,(u_3)^2} = \frac{1}{4}h_\Lambda(u)$$

Puting back together everything we obtain the result. $\qquad\square$

Remark 4.1.50. It is worth noticing that the convex body Λ also appears, up to a multiple, in [BL16, Section 5.1] where it is called $D(2)$, with no apparent link to fiber bodies. In the case where $u_2 \neq 0$ we have

$$h_\Lambda(u) = |u_2|E\left(\sqrt{1-\left(\frac{u_3}{u_2}\right)^2}\right)$$

where $E(s) = \int_0^{\pi/2}\sqrt{1-s^2\sin(\theta)^2}\mathrm{d}\theta$ is the so called complete elliptic integral of the second kind. This function is not semialgebraic thus the example of the dice shows that the fiber body of a semialgebraic convex body is not necessarily semialgebraic. However E is holonomic. This suggests that the curved assumption in Corollary 4.1.27 may not be needed.

4.2. Intersection Bodies of Polytopes

In convex geometry it is common to use functions in order to describe a convex body, i.e. a non-empty convex compact subset of $\mathbb{R}^d$. This can be done e.g. by the radial function. A more detailed introduction can be found in [Sch13].

Definition 4.2.1. Given a convex body $K \subset \mathbb{R}^d$, the *radial function* of K is

$$\rho_K : \mathbb{R}^d \to \mathbb{R}, \quad x \mapsto \max\left\{\lambda \in \mathbb{R} \mid \lambda x \in K\right\}.$$

As a convention $\rho_K(0)$ is ∞ when $0 \in K$ and it is 0 otherwise. An immediate consequence of the definition is that $\rho_K(cx) = \frac{1}{c}\rho_K(x)$ for $c > 0$. Therefore, we can equivalently define the radial function on the unit sphere S^{d-1}, and then extend to the whole space using the previously mentioned relation. Throughout this paper we will use the following convention: x denotes a vector in $\mathbb{R}^d$ whereas u denotes a vector in S^{d-1}. With the observation that we can restrict to the sphere, we define the intersection body of K by its radial function, which is given by the volume of the intersections of K with hyperplanes through the origin.

Definition 4.2.2. Let K be a convex body in $\mathbb{R}^d$. Its *intersection body* is defined to be the set $IK = \{x \in \mathbb{R}^d \mid \rho_{IK}(x) \geq 1\}$ where the radial function (restricted to the sphere) is

$$\rho_{IK}(u) = \mathrm{Vol}_{d-1}(K \cap u^\perp)$$

for $u \in S^{d-1}$. We denote by $u^\perp$ the hyperplane through the origin with normal vector u, and by vol_i the i-dimensional Euclidean volume, for $i \leq d$.
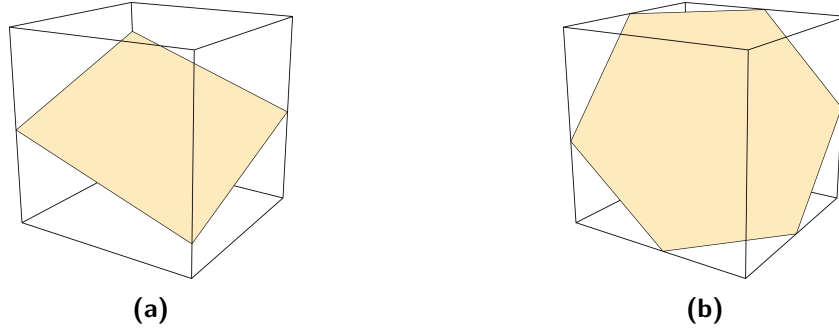
Figure 4.6: The two combinatorial types of hyperplane sections of the 3-cube.

We begin our investigation by considering the intersection body of polytopes which contain the origin. If the origin belongs to the interior of the polytope P, then ρ_P is continuous and hence ρ_{IP} is also continuous [Gar06]. Otherwise we may have some points of discontinuity which correspond to unit vectors u such that $u^\perp$ contains a facet of P; there are finitely many such directions. The intersection body is well defined, but there may arise subtleties when dealing with the boundary. However, we will see later (in 4.2.12) that for our purposes everything works out. In the following we use notions from polytope theory, such as *zonotopes* and *combinatorial types*. For further background on polytopes we refer the reader to [Zie12].

Example 4.2.3. We will use the cube as an ongoing example to illustrate the key concepts used throughout the paper. Let P be the 3-dimensional cube $[-1, 1]^3 \subseteq \mathbb{R}^3$. If we intersect P with hyperplanes $u^\perp$, for $u \in S^2$, we can observe that there are two possible combinatorial types for $P \cap u^\perp$: it is either a parallelogram (4.6a) or a hexagon (4.6b). There are finitely many regions of the sphere for which the combinatorial type stays the same (see 4.2.4). Using this we can parameterize the area of the parallelogram or hexagon with respect to the vector u to construct the radial function of IP. Indeed, as will be shown in the proof of 4.2.6, this can be equivalently written to provide a semialgebraic description of the intersection body. In particular, if the intersection is a square, then the radial function in a neighborhood of that point will be a constant term over a coordinate variable, e.g. $\frac{4}{z}$. On the other hand, when the intersection is a hexagon, the radial function is a degree two polynomial over *xyz*. The intersection body is convex as promised by the theory and displayed in 4.9a. We continue with this in 4.2.13.

◆

Lemma 4.2.4. Let P be a full-dimensional polytope in $\mathbb{R}^d$. Then there exists a central hyperplane arrangement H in $\mathbb{R}^d$ whose maximal open chambers C satisfy the following property. For all $x \in C$, the hyperplane $x^\perp$ intersects a fixed set of edges of P and the polytopes $Q = P \cap x^\perp$ are of the same combinatorial type.

Proof. Let x be a generic vector of $\mathbb{R}^d$ and consider $Q = P \cap x^\perp$. The vertices of Q are the points of intersection of $x^\perp$ with the edges of P. Perturbing x continuously, the intersecting edges (and thus the combinatorial type) remain the same, unless the hyperplane $x^\perp$ passes through a vertex v of P. This happens if and only if $\langle x, v \rangle = 0$ and thus the set of normal vectors of such hyperplanes is given by $v^\perp = \{x \in \mathbb{R}^d \mid \langle x, v \rangle = 0\}$. Taking the union over all vertices yields the central hyperplane arrangement

$$H = \{v^\perp \mid v \text{ is a vertex of } P \text{ and } v \text{ is not the origin}\}.$$

Then each open region C of the complement of H contains points x such that $x^\perp$ intersects

a fixed set of edges of P.   □

The proof of 4.2.4 implies that the number of regions we are interested in is the number of chambers of the central hyperplane arrangement H. Let $m = (\#\{v \text{ is a vertex of } P\}/\sim)$ where $v \sim w$ if $v = \pm w$. Then we have an upper bound for such a number:

$$\sum_{j=0}^{d} \binom{m}{j}$$

given by the number of chambers of a generic arrangement [Sta07, Prop. 2.4].

Remark 4.2.5. We note that there are several ways to view the hyperplane arrangement H in 4.2.4. For example, since the vertices of P are the normal vectors of the facets of the dual polytope P°, we can describe H as the collection of linear hyperplanes which are parallel to facets of P°. We also note that H is the normal fan of a zonotope whose edge directions are orthogonal to the hyperplanes of H. The fan Σ induced by the hyperplane arrangement H is the normal fan of the zonotope

$$Z(P) = \sum_{v \text{ is a vertex of } P} [-v, v].$$

We will call this zonotope the *zonotope associated to* P. As will be clarified later in 4.2.19, the dual body of $Z(P)$ plays an important role in the visualization and the combinatorics of the intersection body IP.

Theorem 4.2.6. Let $P \subseteq \mathbb{R}^d$ be a full-dimensional polytope containing the origin. Then IP, the intersection body of P, is semialgebraic.

Proof. Fix a region $U = C \cap S^{d-1}$ for an open cone C from 4.2.4. Then for every $u \in U$ the hyperplane $u^\perp$ intersects P in the same set of edges. Let v be a vertex of $Q = P \cap u^\perp$. Then there is an edge $[a, b]$ of P such that $v = [a, b] \cap u^\perp$. This implies that $v = \lambda a + (1 - \lambda)b$ for some $\lambda \in (0, 1)$ and $\langle v, u \rangle = 0$. From this we get that

$$\lambda = \frac{\langle b, u \rangle}{\langle b - a, u \rangle}$$

which implies that

$$v = \frac{\langle b, u \rangle}{\langle b - a, u \rangle}(a - b) + b = \frac{\langle b, u \rangle a - \langle a, u \rangle b}{\langle b - a, u \rangle}.$$

In this way we express v as a function of u (for fixed a and b). Let $v_1, \dots, v_n$ be the vertices of Q and let $[a_i, b_i]$ be the corresponding edges of P.

We now consider the following triangulation of Q: first, triangulate each facet of Q that does not contain the origin, without adding new vertices (this can always be done e.g. by a regular subdivision using a generic lifting function, cf. [LRS10, Prop. 2.2.4]). For each $(d-2)$-dimensional simplex Δ in this triangulation, consider the $(d-1)$-dimensional simplex $\text{conv}(\Delta, 0)$ with the origin. This constitutes a triangulation $T = \{\Delta_j : j \in J\}$ of Q, in which the origin is a vertex of every simplex.

Restricting to U, the radial function of the intersection body IP in direction u is the volume of Q, and hence given by

$$\rho_{IP}(u) = \text{vol}(Q) = \sum_{j \in J} \text{vol}(\Delta_j).$$

We can thus compute $\rho_{IP}(u)$ as

$$\rho_{IP}(u) = \sum_{j \in J} \frac{1}{(d-1)!} \left| \det \left(M_j(u) \right) \right|,$$

where

$$M_j(u) = \begin{bmatrix} v_{i_1}(u) \\ v_{i_2}(u) \\ \vdots \\ v_{i_{d-1}}(u) \\ u \end{bmatrix} = \begin{bmatrix} \frac{\langle b_{i_1}, u \rangle a_{i_1} - \langle a_{i_1}, u \rangle b_{i_1}}{\langle b_{i_1} - a_{i_1}, u \rangle} \\ \vdots \\ \frac{\langle b_{i_{d-1}}, u \rangle a_{i_{d-1}} - \langle a_{i_{d-1}}, u \rangle b_{i_{d-1}}}{\langle b_{i_{d-1}} - a_{i_{d-1}}, u \rangle} \\ u \end{bmatrix}$$

and the row vectors $\{v_{i_1}, v_{i_2}, \ldots, v_{i_{d-1}}\}$ (along with the origin) are vertices of the simplex Δ_j of the triangulation. Therefore, we obtain an expression $\rho_{IP}(u) = \frac{p(u)}{q(u)}$ for some polynomials $p, q \in \mathbb{R}[u_1, \ldots, u_d]$ without common factors, for $u \in U$. With the same procedure applied to all regions $U_i = C_i \cap S^{d-1}$, for C_i as in 4.2.4, we obtain an expression for $\rho|_{S^{d-1}}$ that is continuous and piecewise a quotient of two polynomials p_i, q_i. It follows from the definition of the radial function that

$$IP = \left\{ x \in \mathbb{R}^d \mid \rho_{IP}(x) \geq 1 \right\} = \left\{ x \in \mathbb{R}^d \mid \frac{1}{\|x\|} \rho_{IP}\left(\frac{x}{\|x\|} \right) \geq 1 \right\}.$$

Notice that for every $j \in J$ we have the following equality:

$$\det \left(M_j \left(\frac{x}{\|x\|} \right) \right) = \det \begin{bmatrix} v_{i_1}\left(\frac{x}{\|x\|} \right) \\ \vdots \\ v_{i_{d-1}}\left(\frac{x}{\|x\|} \right) \\ \frac{x}{\|x\|} \end{bmatrix} = \det \begin{bmatrix} v_{i_1}(x) \\ \vdots \\ v_{i_{d-1}}(x) \\ \frac{x}{\|x\|} \end{bmatrix} = \frac{1}{\|x\|} \det \left(M_j(x) \right)$$

and therefore, if $\frac{x}{\|x\|} \in U$,

$$\rho_{IP}\left(\frac{x}{\|x\|} \right) = \sum_{j \in J} \frac{1}{(d-1)!} \left| \det \left(M_j \left(\frac{x}{\|x\|} \right) \right) \right| = \frac{1}{\|x\|} \sum_{j \in J} \frac{1}{(d-1)!} \left| \det \left(M_j(x) \right) \right| = \frac{p(x)}{\|x\| q(x)}.$$

Because the radial function is a semialgebraic map, by quantifier elimination the intersection body is also semialgebraic. More explicitly, let I be the set of indices i such that $\rho_{IP}|_{U_i} \neq 0$. Then we can write the intersection body as

$$IP = \bigcup_{i \in I} \left\{ x \in \overline{C}_i \mid \frac{1}{\|x\|^2} \cdot \frac{p_i(x)}{q_i(x)} \geq 1 \right\}$$

$$= \bigcup_{i \in I} \left\{ x \in \overline{C}_i \mid \|x\|^2 q_i(x) - p_i(x) \leq 0 \right\}.$$

This expression gives exactly a semialgebraic description of IP. $\qquad\qquad\square$

Example 4.2.7. Let P be the regular icosahedron in $\mathbb{R}^3$, whose 12 vertices are all the even permutations of $\left(0, \pm\frac{1}{2}, \pm(\frac{1}{4}\sqrt{5} + \frac{1}{4}) \right)$. The associated hyperplane arrangement has $32 = 12 + 20$ chambers. The first type of chambers is spanned by five rays and the radial function of IP is given by a quotient of a quartic and a quintic, defined over $\mathbb{Q}(\sqrt{5})$. In the remaining twenty chambers ρ_{IP} is a quintic over a sextic, again with coefficients in $\mathbb{Q}(\sqrt{5})$. This intersection body is the convex set shown in 4.7. We will continue the analysis of IP in 4.2.20. $\qquad\qquad\blacklozenge$

The theory of intersection bodies assures that the intersection body of a centrally symmetric convex body is again a centrally symmetric convex body, as it happens in 4.2.3 and in 4.2.7. On the other hand, given any polytope P (indeed this holds more generally for any convex body) there exists a translation of P such that IP is not convex. This is the content of the next example.

Example 4.2.8. Let P be the cube $[-1,1]^3 + (1,1,1)$, so that the origin is a vertex of P. The hyperplane arrangement associated to P divides the space in 32 chambers. In two of them the radial function is 0. In six regions the radial function has the following shape (up to permutation of the coordinates and sign):

$$\rho(x,y,z) = \frac{4}{z}.$$

There are then $18 = 6 + 12$ regions in which the radial function looks like

$$\rho(x,y,z) = \frac{2x}{yz} \qquad \text{or} \qquad \rho(x,y,z) = \frac{2(x+2z)}{yz}.$$

In the remaining six regions we have

$$\rho(x,y,z) = \frac{2(x^2 + 2xy + y^2 + 2xz + z^2)}{xyz}.$$

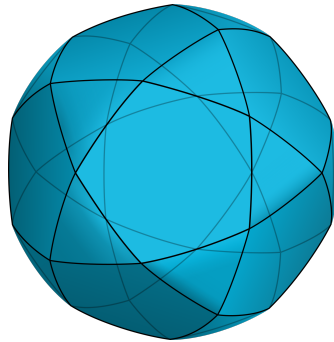4.8 shows two different points of view of IP, which is in particular not convex.   ♦

4.2.1. The role of the origin

The proof of 4.2.6 relies on the fact that the origin is in the polytope. However, if the origin is not contained in P, we can still find a semialgebraic description of IP by adjusting how we compute the volume of $P \cap u^\perp$. The remainder of this section will be dedicated to proving this.
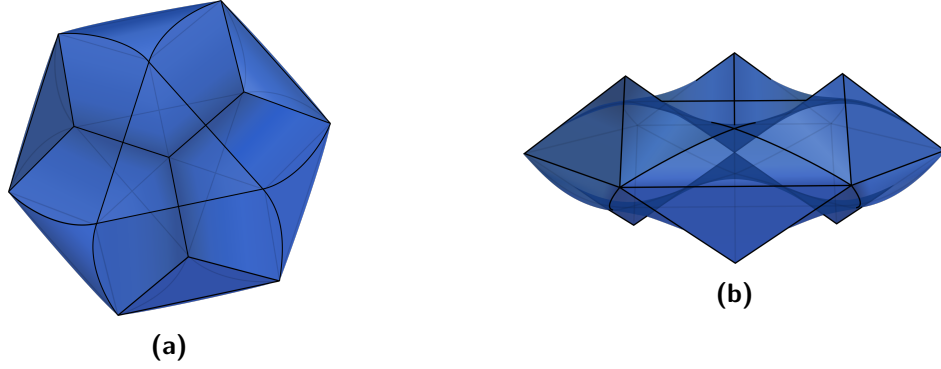
Lemma 4.2.9. Let $P \subset \mathbb{R}^d$ be a full-dimensional polytope, and let $\mathcal{F}$ be the set of its facets. Let p be a point outside of P. For each face $F \in \mathcal{F}$, let $\hat{F}$ denote the set $\mathrm{conv}(F \cup \{p\})$. Then the following equality holds:

$$\mathrm{vol}(P) = \sum_{F \in \mathcal{F}} \mathrm{sgn}(F)\, \mathrm{vol}(\hat{F})$$

where $\mathrm{sgn}(F)$ is 1 if P and p belong to the same halfspace defined by F, and -1 otherwise.

Figure 4.7: The intersection body of the icosahedron.

(b)

(a)

Figure 4.8: The intersection body of the cube in 4.2.8 from two different points of view.

Proof. Let $\hat{P} = \mathrm{conv}(P \cup \{p\})$ and denote by $\mathcal{F}_p^+$ the set of facets F of P for which the halfspace defined by F containing P also contains p, possibly on its boundary. Let $\mathcal{F}_p^- = \mathcal{F} \setminus \mathcal{F}_p^+$.

First we will show that $\hat{P} = \bigcup_{F \in \mathcal{F}_p^+} \hat{F}$. The inclusion $\bigcup_{F \in \mathcal{F}_p^+} \hat{F} \subseteq \hat{P}$ follows immediately from convexity. To see the opposite direction, let $q \in \hat{P}$ and consider r to be the ray starting at p and going through q. Either r intersects P only along its boundary, or there are some intersection points also in the interior of P. In the first case $r \cap P \subset F$ and so $q \in \hat{F}$ for some face F, that by convexity must be in $\mathcal{F}_p^+$. On the other hand, if the ray r intersects the interior of the polytope P, denote by a the farthest among the intersection points:

$$\|a - p\| = \max\{\|\alpha - p\| \mid \alpha \in P \cap r\}.$$

Let F_a be a facet containing a. Then, q is contained in the convex hull of $F_a \cup \{p\}$, i.e. $\hat{F}_a$. From the definition of a it follows that the halfspace defined by F_a containing p must also contain P, so $F_a \in \mathcal{F}_p^+$ and our statement holds.

Next, we will show that $\bigcup_{F \in \mathcal{F}_p^-} \hat{F} = \overline{\hat{P} \setminus P}$. The pyramid $\hat{F}$ is contained in the closed halfspace defined by F which contains p. By the definition of $\mathcal{F}_p^-$, this halfspace does not contain P thus $\hat{F} \cap P = F$. Also, $\hat{F} \subseteq \hat{P}$ so we have that $\hat{F} \subseteq \overline{\hat{P} \setminus P}$ and hence $\bigcup_{F \in \mathcal{F}_p^-} \hat{F} \subseteq \overline{\hat{P} \setminus P}$. Conversely, let $q \in \overline{\hat{P} \setminus P}$. If $q = p$ we are done, so assume $q \neq p$. Then, $q = \lambda p + (1 - \lambda)b$ for some $b \in P$, $\lambda \in [0, 1)$. Let a be the point at which the segment from p to b first intersects the boundary of P, i.e.

$$\|a - p\| = \min\{\|\alpha - p\| \mid \alpha \in P, \alpha = tp + (1 - t)b \text{ for } t \in [0, 1)\}.$$

Then by construction there exists a facet $F_a \in \mathcal{F}_p^-$ containing a, such that $q \in \hat{F}_a$. Thus, we have that

$$\mathrm{vol}(\bigcup_{F \in \mathcal{F}_p^+} \hat{F}) = \mathrm{vol}(\hat{P}) = \mathrm{vol}(\hat{P} \setminus P) + \mathrm{vol}(P) = \mathrm{vol}(\bigcup_{F \in \mathcal{F}_p^-} \hat{F}) + \mathrm{vol}(P).$$

If $F_1 \neq F_2$ and $F_1, F_2 \in \mathcal{F}_p^+$ or $F_1, F_2 \in \mathcal{F}_p^-$, then the volume of $\hat{F}_1 \cap \hat{F}_2$ is zero, therefore

$$\sum_{F \in \mathcal{F}_p^+} \mathrm{vol}(\hat{F}) = \sum_{F \in \mathcal{F}_p^-} \mathrm{vol}(\hat{F}) + \mathrm{vol}(P)$$

and the claim follows. $\qquad\square$

Theorem 4.2.10. Let $P \subset \mathbb{R}^d$ be a full-dimensional polytope. Then IP, the intersection body of P, is semialgebraic.

Proof. What remains to be shown is that IP is semialgebraic in the case when the origin is not contained in P, and hence it is not contained in any of its sections $Q = P \cap u^{\perp}$. From 4.2.9, with $p = 0 \in \mathbb{R}^d$ we have that

$$\mathrm{vol}(Q) = \sum_{F \text{ facet of } Q} \mathrm{sgn}(F) \, \mathrm{vol}(\hat{F})$$

where $\hat{F}$ is the convex hull of F and the origin. Let $T_F = \{\Delta_j : j \in J_F\}$ be a triangulation of F. We can calculate as in the proof of 4.2.6

$$\mathrm{vol}(\hat{F}) = \sum_{j \in J_F} \frac{1}{(d-1)!} |\det M_j|$$

where M_j is the matrix whose rows are the vertices of the simplex $\Delta_j \in T_F$ and u. We then follow the remainder of the proof of 4.2.6 to see that the intersection body is semialgebraic. $\square$

4.2.2. The Algorithm

The proofs from 4.2.6 and 4.2.10 lead to an algorithm to compute the radial function of the intersection body of a polytope. In this section, we describe the algorithm. By 4.2.5, the regions C in which $\rho(x)|_C = \frac{p(x)}{\|x\|^2 q(x)}$ for fixed polynomials $p(x)$ and $q(x)$ are defined by the normal fan of the zonotope $Z(P)$. First, we compute the radial function for each of these cones individually, by applying 1.

Algorithm 1: Computing the radial function for a fixed region C

INPUT: A full-dimensional polytope P in $\mathbb{R}^d$.
INPUT: A maximal open cone C of the normal fan of $Z(P)$.
OUTPUT: The radial function $\rho(x)$ of the intersection body IP restricted to C.

1: Let $\mathcal{F}$ be the collection of facets of P such that for all $u \in U = C \cap S^{d-1}$ and $F \in \mathcal{F}$ holds: $\dim(F \cap u^{\perp}) = \dim(P) - 2$ and $0 \notin F$.

2: Let $Q = P \cap u^{\perp}, u \in U$. Triangulate $F \cap u^{\perp}$ for $F \in \mathcal{F}$, i.e. all facets of Q not containing the origin. Let $\mathcal{T}$ be the collection of all maximal cells of these triangulations.

3: **for** each cell $\Delta \in \mathcal{T}$ **do**

4:     Let $v_1, \ldots, v_{d-1}$ be the vertices of Δ in orientation-preserving order.

5:     For $i = 1, \ldots, d-1$, let $e_i = \mathrm{conv}(a_i, b_i)$ be the edge of P such that $e_i \cap u^{\perp} = v_i$.

6:     Let $x = (x_1, \ldots, x_n)$ be a vector with indeterminates $x_1, \ldots, x_n$. Let M_{Δ} be the $(d \times d)$-matrix with ith row $\frac{\langle b_i, x \rangle a_i - \langle a_i, x \rangle b_i}{\langle b_i - a_i, x \rangle}$ and last row x.

7:     **if** $\mathrm{conv}(\mathbf{0}, \Delta)$ intersects the interior of P **then**

8:         Define $\mathrm{sgn}(\Delta) = 1$

9:     **else**

10:        Define $\mathrm{sgn}(\Delta) = -1$

11:    **end if**

12: **end for**

13: **return** $\frac{1}{\|x\|^2 (d-1)!} \sum_{\Delta \in \mathcal{T}} \mathrm{sgn}(\Delta) \det(M_{\Delta})$

This algorithm has as output the rational function $\rho(x)|_C = \frac{p(x)}{\|x\|^2 q(x)}$. Iterating over all regions yields the final 2.

Algorithm 2: Computing the radial function of IP

INPUT: A full-dimensional polytope P in $\mathbb{R}^d$.
OUTPUT: The radial function $\rho(x)$ of the intersection body IP.
  1: Let Σ be the polyhedral fan from 4.2.5.
  2: **for** each maximal open region C of Σ **do**
  3:     Compute $\rho|_C$ via 1.
  4: **end for**
  5: **return** $\left(\frac{1}{\|x\|^2 (d-1)!} \sum_{\Delta \in \mathcal{T}} \text{sgn}(\Delta) \det(M_\Delta),\ C \right)$ for $C \in \Sigma$

An implementation of these algorithms for `SageMath 9.2` [Sag21] and `Oscar 0.7.1-DEV` [OSC22] can be found in `https://mathrepo.mis.mpg.de/intersection-bodies`. We note that in step 2 of 1, the implementation uses a regular subdivision of the facets of the polytope Q by lifting the vertices $v_1, \ldots, v_m$ along the moment curve $(t^1, \ldots, t^m)$ with $t = 3$.

4.2.3. Algebraic Boundary and Degree Bound

In order to study intersection bodies from the point of view of real algebraic geometry we need to introduce our main character for this section, the algebraic boundary. For more on the algebraic boundary we refer the reader to [Sin15].

Definition 4.2.11. Let K be any compact subset in $\mathbb{R}^d$, then its *algebraic boundary* $\partial_a K$ is the $\mathbb{R}$-Zariski closure of the Euclidean boundary ∂K.

Knowing the radial function of a convex body K implies knowing its boundary. In fact, when $0 \in \text{int } K$ then $x \in \partial K$ if and only if $\rho_K(x) = 1$ (see 4.2.12 for the other cases). Therefore, using the same notation as in the proof of 4.2.6, we can observe that the algebraic boundary of the intersection body of a polytope is contained in the union of the varieties $\mathcal{V}\left(\|x\|^2 q_i(x) - p_i(x)\right)$. Indeed, we actually know more: as will be proven in 4.2.15, the p_i's are divisible by the polynomial $\|x\|^2$, and hence

$$\partial_a IP = \bigcup_{i \in I} \mathcal{V}\left(q_i(x) - \frac{p_i(x)}{\|x\|^2} \right)$$

because of the assumption made in the proof of 4.2.6 that p_i, q_i do not have common components. That is, these are exactly the irreducible components of the boundary of IP.

Remark 4.2.12. As anticipated in **??** there may be difficulties when computing the boundary of IP in the case where the origin is not in the interior of the polytope P. In particular, x is a discontinuity point of the radial function of IP if and only if $x^\perp$ contains a facet of P. Therefore ρ_{IP} has discontinuity points if and only if the origin lies in the union of the affine linear spans of the facets of P. In this case, there are finitely many rays where the radial function is discontinuous and they belong to $\mathbb{R}^d \setminus (\cup_{i \in I} C_i)$, i.e. to the hyperplane arrangement H. If $d = 2$, these rays disconnect the space, and this implies that we loose part of the (algebraic) boundary of IP: to the set $\{x \in \mathbb{R}^d \mid \rho_{IP}(x) = 1\}$ we need to add segments from the origin to the boundary points in the direction of these rays. However, in higher dimensions the discontinuity rays do not disconnect $\mathbb{R}^d$ so $\{x \in \mathbb{R}^d \mid \rho_{IP}(x) = 1\}$ approaches the region where the radial function is zero continuously except for these finitely many directions. Therefore there are no extra components of the boundary of IP.

Example 4.2.13 (Continuation of 4.2.3, cf. 4.9a). Starting from the radial function of the intersection body of the 3-cube P, computed using 1, we can recover the equations of its algebraic boundary. The Euclidean boundary of this convex body is divided in 14 regions. Among them, 6 arise as the intersection of a convex cone spanned by 4 rays with a hyperplane; they constitute facets, i.e. flat faces of dimension $d-1$, of IP. For example the facet exposed by the vector $(1,0,0)$ is the intersection of $z = 4$ with the convex cone

$$\overline{C}_1 = \mathrm{co}\{(1,0,1),(-1,0,1),(0,1,1),(0,-1,1)\}.$$

In other words, the variety $\mathcal{V}(z-4)$ is one of the irreducible components of $\partial_a IP$. The remaining 8 regions are spanned by 3 rays each, and the polynomial that defines the boundary of IP is a cubic, such as

$$2xyz - 2x^2 - 4xy - 2y^2 - 4xz + 4yz - 2z^2$$

in the region

$$\overline{C}_2 = \mathrm{co}\{(0,1,1),(-1,1,0),(-1,0,1)\}.$$

[THE FOLLOWING HAS TO BE DELETED] These cubics are in fact, up to a change of coordinates, the algebraic boundary of a famous spectrahedron: the elliptope [**?**]. Hence $\partial_a IP$ is the union of 14 irreducible components, six of degree 1 and eight of degree 3. ♦

Remark 4.2.14. In [PSW21] the authors introduce the notion of *patches* of a semialgebraic convex body, with the purpose of mimicking the faces of a polytope. In the case of intersection bodies of polytopes, it is tempting to think that each region of 4.2.4 corresponds to a patch. Indeed, this happens, for example, for the centered 3-cube in 4.2.13. On the other hand, if $P = [-1,1]^3 + (0,0,1)$ then there are 4 regions that define the same patch of the algebraic boundary of IP; therefore there is, unfortunately, no one-to-one correspondence between regions and patches.

Proposition 4.2.15. Using the notation of 4.2.4 and 4.2.10, fix a chamber C of H and let $Q = P \cap u^\perp$ for some $u \in U = C \cap S^{d-1}$. Then the polynomial $\|x\|^2 = x_1^2 + \ldots + x_d^2$ divides $p(x)$ and

$$\deg\left(q(x) - \frac{p(x)}{\|x\|^2}\right) \le f_0(Q).$$

Proof. For the fixed region C, let T be a triangulation of Q with simplices indexed by J. Then the volume of Q is given by

$$\frac{p(x)}{q(x)} = \frac{1}{(d-1)!} \sum_{j \in J} |\det(M_j(x))|$$

where M_j is the matrix as in the proof of 4.2.6. Notice that for each $M = M_j$, we can

rewrite the determinant to factor out a denominator (we also write for simplicity $\Delta = \Delta_j$):

$$
\begin{aligned}
\det(M(x)) &= \sum_{\sigma \in S_d} \operatorname{sgn}(\sigma) \prod_{i=1}^{d} M_{i\sigma(i)} \\
&= \sum_{\sigma \in S_d} \operatorname{sgn}(\sigma) x_{\sigma(d)} \prod_{i=1}^{d-1} \frac{\langle b_i, u \rangle a_{i\sigma(i)} - \langle a_i, u \rangle b_{i\sigma(i)}}{\langle b_i - a_i, u \rangle} \\
&= \prod_{i=1}^{d-1} \frac{1}{\langle b_i - a_i, u \rangle} \sum_{\sigma \in S_d} \operatorname{sgn}(\sigma) x_{\sigma(d)} \prod_{i=1}^{d-1} \left(\langle b_i, u \rangle a_{i\sigma(i)} - \langle a_i, u \rangle b_{i\sigma(i)} \right) \\
&= \left(\prod_{\substack{v_i \in \Delta \\ \text{vertex}}} \frac{1}{\langle b_i - a_i, x \rangle} \right) \cdot \det\left(\hat{M}(x) \right)
\end{aligned}
$$

where

$$
\hat{M}(x) = \begin{bmatrix} \vdots \\ \langle b_i, x \rangle a_i - \langle a_i, x \rangle b_i \\ \vdots \\ x \end{bmatrix}
$$

and the determinant of $\hat{M}(x)$ is a polynomial of degree d in the x_i's. Note that if we multiply $\hat{M}(x) \cdot x$ we obtain the vector $(0, \ldots, 0, x_1^2 + \ldots + x_d^2)$. Hence if $x_1^2 + \ldots + x_d^2 = 0$, then $\hat{M}(x) \cdot x = 0$, i.e. the kernel of $\hat{M}(x)$ is non-trivial and thus $\det \hat{M}(x) = 0$. This implies the containment of the complex varieties $\mathcal{V}(\|x\|^2) \subseteq \mathcal{V}(\det \hat{M}(x))$ and therefore the polynomial $x_1^2 + \ldots + x_d^2$ divides the polynomial $\det \hat{M}(x)$. When we sum over all the simplices in the triangulation T we obtain that

$$
\begin{aligned}
q(x) &= (d-1)! \left(\prod_{\substack{v_i \in \Delta \\ \text{vertex}}} \frac{1}{\langle b_i - a_i, x \rangle} \right) \cdot \left(\prod_{\substack{v_i \notin \Delta \\ \text{vertex}}} \frac{1}{\langle b_i - a_i, x \rangle} \right) \\
&= \prod_{\substack{v_i \in Q \\ \text{vertex}}} \frac{1}{\langle b_i - a_i, x \rangle}
\end{aligned}
$$

and

$$
p(x) = \sum_{j \in J} \left(\left| \det\left(\hat{M}(x) \right) \right| \cdot \prod_{\substack{v_i \notin \Delta \\ \text{vertex}}} \frac{1}{\langle b_i - a_i, x \rangle} \right).
$$

Hence $\deg q \leq f_0(Q)$ and $\deg p \leq f_0(Q) + 1$, so the claim follows. $\qquad\square$

Notice that generically, meaning for the generic choice of the vertices of P, the bound in 4.2.15 is attained, because p and q will not have common factors.

Theorem 4.2.16. Let $P \subset \mathbb{R}^d$ be a full-dimensional polytope with $f_1(P)$ edges. Then the degrees of the irreducible components of the algebraic boundary of IP are bounded from above by

$$
f_1(P) - (d-1).
$$

Proof. We want to prove that $f_0(Q) \leq f_1(P) - (d-1)$, for every $Q = P \cap u^\perp$, $u \in S^{d-1} \setminus H$. By definition, every vertex of Q is a point lying on an edge of P, so trivially $f_0(Q) \leq f_1(P)$. We want to argue now that it is impossible to intersect more than $f_1(P) - (d-1)$ edges of P with our hyperplane $\mathcal{H} = u^\perp$. If the origin is one of the vertices of P, then all the edges that have the origin as a vertex give rise only to one vertex of Q: the origin itself. There are at least d such edges, because P is full-dimensional, and so $f_0(Q) \leq f_1(P) - (d-1)$.

Suppose now that the origin is not a vertex of P, then $\mathcal{H}$ does not contain vertices of P. It divides $\mathbb{R}^d$ in two half spaces $\mathcal{H}_+$ and $\mathcal{H}_-$, and so it divides the vertices of P in two families of k vertices in $\mathcal{H}_+$ and ℓ vertices in $\mathcal{H}_-$. Either k or ℓ are equal to 1, or they are both greater than one. In the first case let us assume without loss of generality that $k = 1$, i.e. there is only one vertex v_+ in $\mathcal{H}_+$. Then pick one vector v_- in $\mathcal{H}_-$: because P is a full-dimensional polytope, there are at least d edges of P with v_- as a vertex. Only one of them may connect v_- to v_+ and therefore the other $d-1$ edges must lie in $\mathcal{H}_-$. This gives $f_0(Q) \leq f_1(P) - (d-1)$.

On the other hand, let us assume that $k, \ell \geq 2$. Then there is at least one edge in $\mathcal{H}_+$ and one edge in $\mathcal{H}_-$. If $d = 3$ these are the $d-1$ edges that do not intersect the hyperplane. For $d > 3$ we reason as follows. Suppose that $\mathcal{H}$ intersects a facet F of P. Then it cannot intersect all the facets of F (i.e. a ridge of P), otherwise we would get $F \subset \mathcal{H}$ which contradicts the fact that $\mathcal{H}$ does not intersect vertices of P. So there exists a ridge F' of P that does not intersect the hyperplane; it has dimension $d - 2 \geq 2$ and therefore it has at least $d - 1$ edges. Therefore

$$f_0(Q) \leq f_1(P) - (d-1).$$

$\square$

Corollary 4.2.17. In the hypotheses of 4.2.16, if P is centrally symmetric and centered at the origin, then we can improve the bound with

$$\frac{1}{2}\left(f_1(P) - (d-1)\right).$$

Proof. We already know that for each chamber C_i from 4.2.4, the degree of the corresponding irreducible component is bounded by the degree of the polynomial q_i. This follows from the construction of p_i and q_i in the proof of 4.2.6. Specifically, the determinant which gives p_i/q_i comes with the product of $d - 1$ rational functions, with linear numerator and denominators, and one linear term. Thus $\deg p_i = \deg q_i + 1$ which implies that $\deg \frac{p_i}{\|x\|^2} < \deg q_i$. By definition these polynomials are obtained as the least common multiple of objects with shape

$$\prod_{\substack{v_k \in \Delta_j \\ \text{vertex}}} \frac{1}{\langle b_k - a_k, x \rangle}.$$

If P is centrally symmetric, so is Q, and therefore we have the vertex belonging to the edge $[a_k, b_k]$ and also the vertex belonging to the edge $[-a_k, -b_k]$. When computing the least common multiple, these two vertices produce the same factor, up to a sign, and therefore they count as the same linear factor of q_i. Hence for every i

$$\deg q_i(x) \leq \frac{f_0(Q)}{2} \leq \frac{1}{2}\left(f_1(P) - (d-1)\right).$$

$\square$

Example 4.2.18. Let P be the tetrahedron in $\mathbb{R}^3$ with vertices $(-1,-1,-1), (-1,1,1), (1,-1,1),$ $(1,1,-1)$. The associated hyperplane arrangement coincides with the one associated to the cube in 4.2.13, so it has 14 chambers that come in two families. The first one consists

(a)   **(b)**   **(c)**
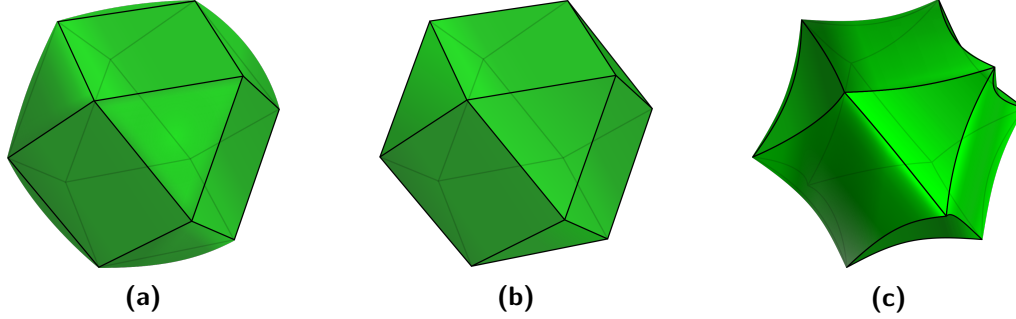
Figure 4.9: Left: the intersection body of the cube in 4.2.13. Right: the intersection body of the tetrahedron in 4.2.18. Center: the dual body of the zonotope $Z(P)$ associated to both the cube and the tetrahedron. Such a polytope reveals the structure of the boundary divided into regions of these two intersection bodies.

of cones spanned by four rays, such as $\overline{C}_1$ (see 4.2.13). The polynomial that defines the boundary of IP in this region is a quartic, namely

$$q_2(x,y,z) - \frac{p_2(x,y,z)}{\|(x,y,z)\|^2} = (x+z)(x-z)(y+z)(y-z) - 2(x^2+y^2-z^2)z.$$

On the other hand the cones of the second family are spanned by three rays: here the section of P is a triangle and the equation of the boundary if IP is a cubic. An example is the cone $\overline{C}_2$ with the polynomial

$$q_1(x,y,z) - \frac{p_1(x,y,z)}{\|(x,y,z)\|^2} = (x-y)(x-z)(y+z) + (x-y-z)^2.$$

Note that this region furnishes an example in which the bounds given in 4.2.15 and 4.2.16 are attained.   ♦

Remark 4.2.19. 4.2.5 together with 4.2.15 implies that the structure of the irreducible components of the algebraic boundary of IP is strongly connected with the face lattice of the dual of the zonotope $Z(P)$. More precisely, in the generic case, the lattice of intersection of the irreducible components is isomorphic to the face lattice of the dual polytope $Z(P)^\circ$. Thus, a classification of "combinatorial types" of such intersection bodies is analogous to the classification of zonotopes / hyperplane arrangements / oriented matroids. It is however worth noting, that the same zonotope can be associated to two polytopes P_1 and P_2 which are not combinatorially equivalent. One example of this instance is a pair of polytopes such that $P_1 = \text{conv}(v_1, \ldots, v_n)$ and $P_2 = \text{conv}(\pm v_1, \ldots, \pm v_2)$, as can be seen in 4.9 for the cube and the tetrahedron. To have a better overview over the structure of the boundary of IP, one strategy is to use the Schlegel diagram of $Z(P)^\circ$. We label each maximal cell by the degree of the polynomial that defines the corresponding irreducible component of ∂IP, as can be seen in **??**.

Example 4.2.20 (Continuation of 4.2.7, cf. 4.7)**.** Let P be the regular icosahedron. In the 12 regions which are spanned by five rays, the polynomial that defines the boundary of
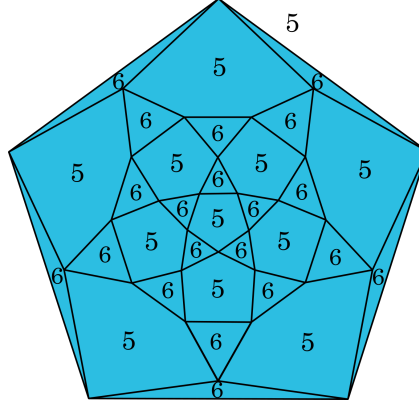
Figure 4.10: The Schlegel diagram of $Z(P)^{\circ}$, in the case where P is the icosahedron from 4.2.20. The labels represent the degrees of the polynomials of $\partial_a IP$.

IP has degree 5 and it looks like

$$((\sqrt{5}x + \sqrt{5}y - x + y)^2 - 4z^2)((\sqrt{5}x + x + 2y)^2 - (\sqrt{5}z - z)^2)y+$$
$$8\sqrt{5}x^3y + 68\sqrt{5}x^2y^2 + 72\sqrt{5}xy^3 + 20\sqrt{5}y^4 - 40\sqrt{5}xyz^2 - 20\sqrt{5}y^2z^2 + 4\sqrt{5}z^4+$$
$$8x^3y + 164x^2y^2 + 168xy^3 + 44y^4 - 8x^2z^2 - 72xyz^2 - 44y^2z^2 + 12z^4.$$

In the other 20 regions spanned by three rays, ∂IP is the zero set of a sextic polynomial with the following shape

$$((\sqrt{5}x + x + 2y)^2 - (\sqrt{5}z - z)^2)((\sqrt{5}y - 2x - y)^2 - (\sqrt{5}z - z)^2)xy + 20\sqrt{5}x^4y-$$
$$20\sqrt{5}x^2y^3 - 4\sqrt{5}xy^4 + 4\sqrt{5}y^5 - 4\sqrt{5}x^3z^2 - 60\sqrt{5}x^2yz^2 - 12\sqrt{5}xy^2z^2 + 12\sqrt{5}xz^4 + 44x^4y-$$
$$8x^3y^2 - 44x^2y^3 + 12xy^4 + 12y^5 - 12x^3z^2 - 156x^2yz^2 - 60xy^2z^2 - 8y^3z^2 + 28xz^4.$$

We visualize the structure of these pieces using the Schlegel diagram in 4.10, where the numbers correspond to the degree of the polynoimals, as explained in 4.2.19.   ♦

Using this technique we are then able to visualize the boundary of intersection bodies of 4-dimensional polytopes via the Schlegel diagram of $Z(P)^{\circ}$.

Example 4.2.21. Let $P = \text{conv}\{(1, 1, 0, 0), (0, 1, 0, 0), (0, -1, 0, 0), (0, 0, -1, 0), (0, 0, 0, -1)\}$. The boundary of its intersection body IP is subdivided in 16 regions. In four of them the equation is given by a polynomial of degree 3, whereas in the remaining twelve regions the polynomial has degree 5. In 4.11 we show the Schlegel diagram of

$$Z(P)^{\circ} = \text{conv}\{\pm(1/2, -1/2, 0, 0), \pm(1, 0, 0, 0), \pm(0, 0, 1, 0), \pm(0, 0, 0, 1)\}$$

with a number associated to each maximal cell which represents the degree of the polynomial in the corresponding region of ∂IP.   ♦

4.2.4. The Cube

In this section we investigate the intersection body of the d-dimensional cube $C^{(d)} = [-1, 1]^d$, with a special emphasis on the linear components of its algebraic boundary.

Proposition 4.2.22. The algebraic boundary of the intersection body of the d-dimensional cube $C^{(d)}$ has at least $2d$ linear components. These components correspond to the $2d$ open regions from 4.2.4 which contain the standard basis vectors and their negatives.
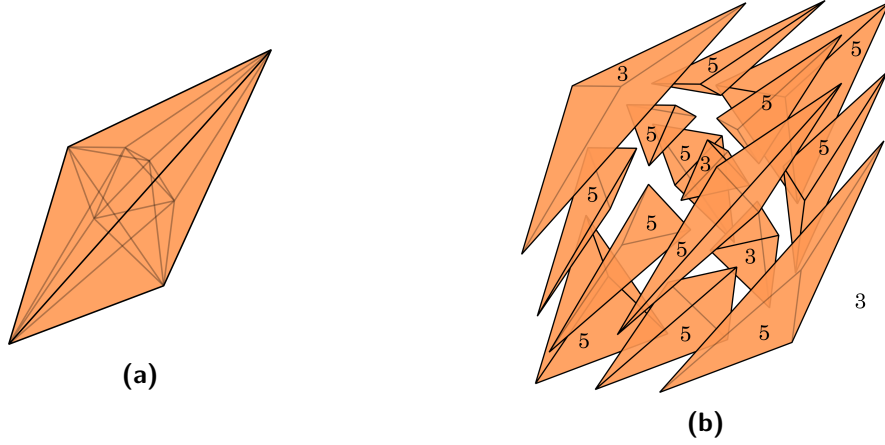
Figure 4.11: The Schlegel diagram of $Z(P)^\circ$ from 4.2.21. There are four cells whose corresponding polynomial in ∂IP has degree 3, including the outer facet; the others correspond to degree 5 polynomials.

Proof. We show the claim for the first standard basis vector e_1. The argument for the other vectors $\pm e_i, i = 1, \ldots, d$ is analogous.

Let C be the region from 4.2.4 which contains e_1 and consider $U = C \cap S^{d-1}$. For any $u \in U$, the polytope $C^{(d)} \cap u^\perp$ is combinatorially equivalent to $C^{(d-1)}$. Hence we can compute the (signed) volume,

$$\mathrm{vol}(C^{(d)} \cap u^\perp) = \det \begin{bmatrix} v^{(1)} - v^{(0)} \\ \vdots \\ v^{(d-1)} - v^{(0)} \\ u \end{bmatrix}$$

where $v^{(0)}$ is an arbitrarily chosen vertex of $C^{(d)} \cap u^\perp$ and the remaining $v^{(i)}$ are vertices of $C^{(d)} \cap u^\perp$ adjacent to $v^{(0)}$. Next, we observe that for any vertex v of $C^{(d)} \cap u^\perp$ which lies on the edge $[a, b]$ of $C^{(d)}$, v is the vector

$$v = \left(-\frac{1}{u_1} \sum_{j=2}^{d} a_j u_j, \ a_2, \ \ldots, \ a_d \right).$$

This follows from the formulation of v in the proof of 4.2.6 and the fact that $b_1 = -a_1$ and $b_i = a_i$ for $i = 2, \ldots, d$. Combining this with the determinant above gives us the following expression for the radial function restricted to U:

$$\rho(u) = \frac{1}{u_1} \det \begin{bmatrix} -\sum_{j=2}^{d}(a_j^{(1)} - a_j^{(0)})u_j & a_2^{(1)} - a_2^{(0)} & \cdots & a_d^{(1)} - a_d^{(0)} \\ -\sum_{j=2}^{d}(a_j^{(2)} - a_j^{(0)})u_j & a_2^{(2)} - a_2^{(0)} & \cdots & a_d^{(2)} - a_d^{(0)} \\ \vdots & \vdots & & \vdots \\ -\sum_{j=2}^{d}(a_j^{(d)} - a_j^{(0)})u_j & a_2^{(d)} - a_2^{(0)} & \cdots & a_d^{(d)} - a_d^{(0)} \\ u_1^2 & u_2 & \cdots & u_d \end{bmatrix}$$

where we assume the determinant is nonnegative, else we will multiply by -1. Expanding

the determinant along the bottom row of the matrix yields

$$\rho(u) = \frac{1}{u_1}\left(u_1^2 \det \begin{bmatrix} a_2^{(1)} - a_2^{(0)} & \dots & a_d^{(1)} - a_d^{(0)} \\ a_2^{(2)} - a_2^{(0)} & \dots & a_d^{(2)} - a_d^{(0)} \\ & \vdots & \\ a_2^{(d)} - a_2^{(0)} & \dots & a_d^{(d)} - a_d^{(0)} \end{bmatrix} + \gamma(u_2, \dots, u_n)\right).$$

where $\gamma(u_2, \dots, u_d)$ is a polynomial consisting of the quadratic terms in the remaining u_i's. Note that since γ does not contain the variable u_1 and ρ is divisible by the quadric $u_1^2 + \dots + u_d^2$ by 4.2.15, it follows that

$$\rho(u) = \frac{u_1^2 + \dots + u_d^2}{u_1} \ \det \begin{bmatrix} a_2^{(1)} - a_2^{(0)} & \dots & a_d^{(1)} - a_d^{(0)} \\ a_2^{(2)} - a_2^{(0)} & \dots & a_d^{(2)} - a_d^{(0)} \\ & \vdots & \\ a_2^{(d)} - a_2^{(0)} & \dots & a_d^{(d)} - a_d^{(0)} \end{bmatrix}. \tag{4.2.1}$$

Let A be the $(d-1) \times (d-1)$-matrix appearing in this last expression (4.2.1). Then finally, by the discussion in 4.2.3, the irreducible component of the algebraic boundary on the corresponding conical region C is described by the linear equation $x_1 = |\det A|$. $\qquad\square$

Note that for an arbitrary polytope P of dimension at least 3, the irreducible components of the algebraic boundary $\partial_a IP$ cannot all be linear. This is implied by the fact that the intersection body of a convex body is not a polytope. It is thus worth noting that the intersection body of the cube has remarkably many linear components. We now investigate the non-linear pieces of $\partial_a IC^{(4)}$ of the 4-dimensional cube.

Example 4.2.23. Let P be the 4-dimensional cube $[-1, 1]^4$ and IP be its intersection body. The associated hyperplane arrangement has $8 + 32 + 64 = 104$ chambers. The first 8 are spanned by 6 rays and the boundary here is linear, i.e. it is a 3-dimensional cube. For example, the linear face exposed by $(1, 0, 0, 0)$ is cut out by the hyperplane $w = 8$.

The second family of chambers is made of cones with 5 extreme rays, where the boundary is defined by a cubic equation with shape

$$3xyz - 3w^2 - 6x^2 - 12xy - 6y^2 - 12xz + 12yz - 6z^2.$$

Finally there are 64 cones spanned by 4 rays such that the boundary of the intersection body is a quartic, such as

$$4wxyz - w^3 - 3w^2x - 3wx^2 - x^3 - 3w^2y - 6wxy - 3x^2y - 3wy^2 - 3xy^2$$
$$- y^3 - 3w^2z - 6wxz - 3x^2z + 18wyz - 6xyz - 3y^2z - 3wz^2 - 3xz^2 - 3yz^2 - z^3.$$

$\blacklozenge$

4.2.22 gives a lower bound on the number of linear components of the algebraic boundary of $IC^{(d)}$. We conjecture that for any $d \in \mathbb{N}$, the algebraic boundary of the intersection body of the d-dimensional cube centered at the origin has exactly $2d$ linear components. Computational results for $d \le 5$ support this conjecture, as displayed in 4.1. It shows the number of irreducible components of $IC^{(d)}$ sorted by the degree of the component, for $d = 2, 3, 4, 5$. The first two columns are the dimension of the polytope, and the number of chambers of the respective hyperplane arrangement H. The third column is the degree

dimension	# chambers	degree bound	deg = 1	2	3	4	5
2	4	1	4	0	0	0	0
3	14	5	6	0	8	0	0
4	104	14	8	0	32	64	0
5	1882	38	10	0	80	320	1472

Table 4.1: Number of irreducible components of the algebraic boundary of the intersection body of the d-cube, listed by degree.

bound from 4.2.17. The remaining columns show the number of regions whose equation in the algebraic boundary have degree deg, for deg $= 2, \ldots, 5$.

It is worth noting that the highest degree attained in these examples is equal to the dimension of the respective cube. In particular, the degree bound for centrally symmetric polytopes, as given in 4.2.17 is not attained in any of the cases for $d \geq 3$. Finally, note that the number of regions grows exponentially in d, and thus for $d \geq 3$, the number of non-linear components exceeds the number of linear components.

Chapter 5

The Convex Hull of Surfaces in 4-space

Chapter 6

Convex Bodies in Applications: Quantum Physics

Bibliography

[ADRS00] Christos A. Athanasiadis, Jesús A. De Loera, Victor Reiner, and Francisco Santos. Fiber polytopes for the projections between cyclic polytopes. *European Journal of Combinatorics*, 21(1):19–47, 2000.

[AS16]   Karim A. Adiprasito and Raman Sanyal. Whitney numbers of arrangements via measure concentration of intrinsic volumes. *arXiv:1606.09412*, 2016.

[Aum65] Robert J. Aumann. Integrals of set-valued functions. *Journal of Mathematical Analysis and Applications*, 12(1):1–12, 1965.

[Bar02] Alexander Barvinok. *A course in convexity*, volume 54 of *Graduate Studies in Mathematics*. American Mathematical Society, 2002.

[BL16]   Peter Bürgisser and Antonio Lerario. Probabilistic schubert calculus. *Journal für die reine und angewandte Mathematik (Crelles Journal)*, 2020:1 – 58, 2016.

[BL21]   Alexander Black and Jesús De Loera. Monotone paths on cross-polytopes. *arXiv:2102.01237*, 2021.

[BS92]   Louis J. Billera and Bernd Sturmfels. Fiber polytopes. *Annals of Mathematics*, 135(3):527–549, 1992.

[Cam99] Stefano Campi. Convex intersection bodies in three and four dimensions. *Mathematika*, 46(1):15–27, 1999.

[CKLS19] Daniel Ciripoi, Nidhi Kaihnsa, Andreas Löhne, and Bernd Sturmfels. Computing convex hulls of trajectories. *Rev. Un. Mat. Argentina*, 60(2):637–662, 2019.

[CSM03] David Cohen-Steiner and Jean-Marie Morvan. Restricted Delaunay triangulations and normal cycle. In *Proceedings of the nineteenth annual symposium on Computational geometry*, pages 312–321, 2003.

[EK08]   Alexander Esterov and Askold Khovanskii. Elimination theory and newton polytopes. *Functional Analysis and Other Mathematics*, 2(1):45–71, 2008.

[Est08] Aleksandr Esterov. On the existence of mixed fiber bodies. *Moscow Mathematical Journal*, 8(3):433–442, 2008.

[Fed59] Herbert Federer. Curvature measures. *Trans. Amer. Math. Soc.*, 93:418–491, 1959.

[Fu14]   Joseph HG Fu. Algebraic integral geometry. In E. Gallego and G. Solanes, editors, *Integral geometry and valuations*, pages 47–112. Springer, 2014.

[Gar94a] Richard J. Gardner. Intersection bodies and the Busemann-Petty problem. *Trans. Amer. Math. Soc.*, 342(1):435–445, 1994.

[Gar94b] Richard J. Gardner. A positive answer to the Busemann-Petty problem in three dimensions. *Ann. of Math. (2)*, 140(2):435–447, 1994.

[Gar06] Richard J. Gardner. *Geometric Tomography*, volume 58 of *Encyclopedia of Mathematics and its Applications*. Cambridge University Press, New York, second edition, 2006.

[GKS99] Richard J. Gardner, Alexander Koldobsky, and Thomas Schlumprecht. An analytic solution to the Busemann-Petty problem on sections of convex bodies. *Ann. of Math. (2)*, 149(2):691–703, 1999.

[HHMM20] Guillermo Hansen, Irmina Herburt, Horst Martini, and Maria Moszyńska. Starshaped sets. *Aequationes Mathematicae*, 94(6):1001–1092, 2020.

[Kho12] Askold Khovanskii. Completions of convex families of convex bodies. *Mathematical Notes*, 91, 2012.

[KM40] M. G. Kreĭn and D P Milman. On extreme points of regular convex sets. *Studia Mathematica*, 9:133–138, 1940.

[Kol98] Alexander Koldobsky. Intersection bodies, positive definite distributions, and the Busemann-Petty problem. *Amer. J. Math.*, 120(4):827–840, 1998.

[LRS10] Jesus De Loera, Joerg Rambau, and Francisco Santos. *Triangulations*. Springer-Verlag GmbH, August 2010.

[Lud06] Monika Ludwig. Intersection bodies and valuations. *Amer. J. Math.*, 128(6):1409–1428, 2006.

[Lut88] Erwin Lutwak. Intersection bodies and dual mixed volumes. *Adv. in Math.*, 71(2):232–261, 1988.

[Mar94] Horst Martini. Cross-sectional measures. In *Intuitive Geometry (Szeged, 1991)*, volume 63 of *Colloq. Math. Soc. János Bolyai*, pages 269–310. North-Holland, Amsterdam, 1994.

[Mat21] MATHREPO Mathematical data and software. `https://mathrepo.mis.mpg.de/intersection-bodies`, 2021. [Online; accessed 20-December-2021].

[OSC22] Oscar – open source computer algebra research system, version 0.8.1-dev, 2022.

[PSW21] Daniel Plaumann, Rainer Sinn, and Jannik Lennart Wesner. Families of faces and the normal cycle of a convex semi-algebraic set. *arXiv:2104.13306*, 2021.

[Ren06] James Renegar. Hyperbolic programs, and their derivative relaxations. *Foundations of Computational Mathematics*, 6:59–79, 02 2006.

[RG17] Pierre Roussillon and Joan Alexis Glaunès. Surface matching using normal cycles. In *International Conference on Geometric Science of Information*, pages 73–80. Springer, 2017.

[Sag21] The Sage Developers. *SageMath, the Sage Mathematics Software System (Version 9.2)*, 2021. `https://www.sagemath.org`.

[San13]   Raman Sanyal. On the derivative cones of polyhedral cones. *Advances in Geometry*, 13(2):315–321, 2013.

[Sch13]   Rolf Schneider. *Convex Bodies: The Brunn–Minkowski Theory*. Encyclopedia of Mathematics and its Applications. Cambridge University Press, 2 edition, 2013.

[Sin15]   R. Sinn. Algebraic Boundaries of Convex Semi-Algebraic Sets. *Research in the Mathematical Sciences*, 2(1), 2015.

[SLC$^+$19]   Kehua Su, Na Lei, Wei Chen, Li Cui, Hang Si, Shikui Chen, and Xianfeng Gu. Curvature adaptive surface remeshing by sampling normal cycle. *Computer-Aided Design*, 111:1–12, 2019.

[SS19]   Anna-Laura Sattelberger and Bernd Sturmfels. D-modules and holonomic functions. *arXiv:1910.01395*, 2019.

[Sta07]   Richard Stanley. An introduction to hyperplane arrangements. In *Geometric Combinatorics*, pages 389–496. American Mathematical Society, October 2007.

[SY08]   Bernd Sturmfels and Josephine Yu. Tropical implicitization and mixed fiber polytopes. In *Software for algebraic geometry*, pages 111–131. Springer, 2008.

[Vit91]   Richard A. Vitale. Expected absolute random determinants and zonoids. *Ann. Appl. Probab.*, 1(2):293–300, 05 1991.

[Win82]   Peter Wintgen. Normal cycle and integral curvature for polyhedra in Riemannian manifolds. In Gy. Soos and J. Szenthe, editors, *Differential Geometry*, volume 21. North-Holland, Amsterdam, 1982.

[Zäh86]   Martina Zähle. Integral and current representation of Federer's curvature measures. *Arch. Math.*, 46:557–567, 1986.

[Zha99a]   Gaoyong Zhang. Intersection bodies and polytopes. *Mathematika*, 46(1):29–34, 1999.

[Zha99b]   Gaoyong Zhang. A positive solution to the Busemann-Petty problem in $\mathbb{R}^4$. *Ann. of Math. (2)*, 149(2):535–543, 1999.

[Zie12]   Günter M Ziegler. *Lectures on polytopes*, volume 152. Springer Science & Business Media, 2012.

Selbstständigkeitserklärung

Hiermit erkläre ich, die vorliegende Dissertation selbständig und ohne unzulässige fremde Hilfe angefertigt zu haben. Ich habe keine anderen als die angeführten Quellen und Hilfsmittel benutzt und sämtliche Textstellen, die wörtlich oder sinngemäß aus veröffentlichten oder unveröffentlichten Schriften entnommen wurden, und alle Angaben, die auf mündlichen Auskünften beruhen, als solche kenntlich gemacht. Ebenfalls sind alle von anderen Personen bereitgestellten Materialien oder erbrachten Dienstleistungen als solche gekennzeichnet.

Leipzig, den March 14, 2022

. . . .
(Chiara Meroni)

Daten zum Autor

Name:	Chiara Meroni
Geburtsdatum:	22.01.1996 in Gorizia (Italien)
10/2015 - 7/2018	B.Sc. in Mathematik
	Universität Trieste
10/2018 - 7/2020	M.Sc. in Mathematik
	Universität Trieste
seit 10/2020	Doktorandin der Mathematik